

ISTANBUL TECHNICAL UNIVERSITY ★ GRADUATE SCHOOL OF SCIENCE
ENGINEERING AND TECHNOLOGY

**BEHAVIORAL CLASSIFICATION OF STOCHASTIC
DIFFERENTIAL EQUATIONS IN MATHEMATICAL FINANCE**

Ph.D. THESIS

Burhaneddin İZGİ

Department of Mathematical Engineering

Mathematical Engineering Programme

JULY 2015

ISTANBUL TECHNICAL UNIVERSITY ★ GRADUATE SCHOOL OF SCIENCE
ENGINEERING AND TECHNOLOGY

**BEHAVIORAL CLASSIFICATION OF STOCHASTIC
DIFFERENTIAL EQUATIONS IN MATHEMATICAL FINANCE**

Ph.D. THESIS

Burhaneddin İZGİ
(509102001)

Department of Mathematical Engineering

Mathematical Engineering Programme

Thesis Advisor: Assoc. Prof. Dr. Ahmet DURAN

JULY 2015

İSTANBUL TEKNİK ÜNİVERSİTESİ ★ FEN BİLİMLERİ ENSTİTÜSÜ

**MATEMATİKSEL FİNANSTAKİ STOKASTİK
DİFERANSİYEL DENKLEMLERİN DAVRANIŞSAL SINIFLANDIRMASI**

DOKTORA TEZİ

**Burhaneddin İZGİ
(509102001)**

Matematik Mühendisliği Anabilim Dalı

Matematik Mühendisliği Programı

Tez Danışmanı: Doç. Dr. Ahmet DURAN

TEMMUZ 2015

Burhaneddin İZGİ, a Ph.D. student of ITU Graduate School of ScienceEngineering and Technology 509102001 successfully defended the thesis entitled “BEHAVIORAL CLASSIFICATION OF STOCHASTIC DIFFERENTIAL EQUATIONS IN MATHEMATICAL FINANCE”, which he/she prepared after fulfilling the requirements specified in the associated legislations, before the jury whose signatures are below.

Thesis Advisor : **Assoc. Prof. Dr. Ahmet DURAN**
Istanbul Technical University

Jury Members : **Prof. Dr. İsmail KÖMBE**
Istanbul Commerce University

Assoc. Prof. Dr. Koray Deniz ŞİMŞEK
Sabancı University

Asst. Prof. Dr. Bahri GÜLDOĞAN
Istanbul Technical University

Asst. Prof. Dr. Cihangir ÖZEMİR
Istanbul Technical University

Date of Submission : **10 June 2015**

Date of Defense : **14 July 2015**

To my wife AYÇA and my sweet daughter İKRA BÜŞRA

FOREWORD

This dissertation is dedicated with greatest respects and gratitudes to my father M. Emin İzgi, to my mother Şükran İzgi, to my wife Ayça İzgi and to my sweet daughter İkra Büşra. Many special thanks go out to them for their understanding, supporting, warm behaviors and unconditional believe in me at any time of my life.

I am sincerely grateful for the support and encouragement of my family, particularly, my brother Burak, sister Esra, sister-in-law Hatice, brother-in-law Taner, father-in-law Lütfü, mother-in-law Leyla and aunt Aynur Altun.

I would like to thank to my esteemed advisor Assoc. Prof. Dr. Ahmet Duran for his assistance, encouragement, patience and guidance during my PhD studies. I'd like to present my gratitudes to him for his confidence in me.

I would also like to thank to the Doctoral committee members Assist. Prof. Dr. Bahri Göldoğan from Istanbul Technical University and Assoc. Prof. Dr. Koray Deniz Şimşek from Sabancı University for their supportive and valuable comments and suggestions.

I owe many thanks and respects to Assoc. Prof. Dr. Coşkun Çetin and all members of the Department of Mathematics and Statistics at California State University, Sacramento in USA for their assistance and hospitality during my research as a visiting researcher in 2014.

My final thanks goes out to my friend İlhan Gül and all members of the Department of Mathematics Engineering at Istanbul Technical University for their help and sincerity.

The support of The Scientific and Technological Research Council of Turkey (TUBITAK) is gratefully acknowledged throughout my PhD education.

July 2015

Burhaneddin İZGİ

TABLE OF CONTENTS

	<u>Page</u>
FOREWORD.....	ix
TABLE OF CONTENTS.....	xi
ABBREVIATIONS	xiii
LIST OF TABLES	xv
LIST OF FIGURES	xvii
SUMMARY	xix
ÖZET	xxi
1. INTRODUCTION	1
1.1 Basic Stochastic Differential Equations	1
1.1.1 Merton-Black Scholes model	3
1.1.2 Merton's jump diffusion model	3
1.1.3 Heston stochastic volatility model.....	4
1.2 Numerical Methods	5
1.2.1 Euler Maruyama method	5
1.2.2 Milstein method.....	6
1.2.3 Stochastic Runge-Kutta method	6
1.3 Stochastic Calculus for Jump Process	7
1.3.1 Itô-Doebelin formula for jump process	7
1.3.2 Simulation strategy of the jump process	9
2. APPLICATION OF HESTON MODEL FOR BORSA ISTANBUL	13
2.1 3-Dimensional Matrix Norms.....	14
2.2 Impression Matrix Norm	16
2.3 Simulations Results	18
2.3.1 Scenarios: Randomly generated interest rates.....	18
2.3.2 Volatility in terms of extreme values	20
2.3.3 Real data applications	21
3. EXTREME VALUE ANALYSIS AND ITS APPLICATION IN FINANCE	27
3.1 Application of Extreme Value Theory on Heston Model.....	27
3.1.1 Extreme value theory.....	28
3.1.2 High peak and fat tail analysis for the model parameters	29
3.2 High Peak and Fat Tail Analysis for BIST-100	37
3.3 3D Dynamics of the Average Logarithmic Stock Return, Interest Rate and Speed of Mean Reversion Variables	40
3.4 Comovement and Polarization of Interest Rates and Daily Returns	42
4. JUMP DIFFUSION VS MERTON-BLACK SCHOLES MODELS.....	45
4.1 Behavioral Comparisons of Merton Jump Diffusion and Merton-Black Scholes Models.....	45

4.1.1 Extensive behavioral analysis of the jump 47

4.2 Summary of the Extensive Behavioral Analyses..... 52

4.3 Application of Impression Matrix Norm for Jump Process 55

5. CONCLUSIONS AND RECOMMENDATIONS..... 57

REFERENCES..... 61

CURRICULUM VITAE..... 66

ABBREVIATIONS

SDE	: Stochastic Differential Equation
MBS	: Merton-Black Scholes
MJD	: Merton's Jump Diffusion
CIR	: Cox, Ingersoll and Ross
SRK	: Stochastic Runge-Kutta
CN	: Compensated Poisson Process
QQ	: Quantile-quantile
ME	: Mean Excess
BIST-100	: Borsa Istanbul - 100
2D	: 2-dimensional
3D	: 3-dimensional
EMH	: Efficient Market Hypothesis
IMN	: Impression Matrix Norm

LIST OF TABLES

	<u>Page</u>
Table 2.1 : Simulation parameters.....	17
Table 2.2 : Parameters for different interest rates scenarios.....	19
Table 2.3 : Average values of norms obtained by using randomly generated interest rates.	21
Table 2.4 : Volatilities in terms of extreme values.	21
Table 2.5 : Average values of norms obtained by using the annual volatility at the overlapping case.....	24
Table 2.6 : Average values of norms obtained by using the daily volatility at the overlapping case.....	24
Table 3.1 : Daily volatilities and variances in terms of extreme values.	30
Table 3.2 : Statistics for distributions of logarithmic stock return for positive correlation coefficient.	32
Table 3.3 : Statistics for distributions of logarithmic stock return for negative correlation coefficient.	32
Table 3.4 : Statistics for distribution of daily logarithmic BIST-100 returns, 2004 - 2013.	37
Table 4.1 : MBS: Statistics for the distribution of logarithmic stock price.....	52
Table 4.2 : MJD: Statistics for the distributions of logarithmic stock price for μ_X while $\sigma_X = 1$	53
Table 4.3 : MJD: Statistics for the distributions of logarithmic stock price for σ_X while $\mu_X = 0$	53

LIST OF FIGURES

	<u>Page</u>
Figure 2.1 : One thousand realizations of simulation when $r = 7.5\%$, $v_0 = 119 \times 10^{-7}$ and $\theta = 52 \times 10^{-7}$	17
Figure 2.2 : One thousand realizations of simulation for second scenario.....	19
Figure 2.3 : Impression norm of matrix M for second scenario by Euler - Maruyama method.	20
Figure 2.4 : Impression norm of matrix M for second scenario by Milstein method.....	20
Figure 2.5 : Impression norm of matrix M for second scenario by stochastic Runge-Kutta method.....	20
Figure 2.6 : Daily interest returns between 02.01.2012 and 31.12.2012.....	22
Figure 2.7 : Impression norm of matrix M for daily volatility by Euler - Maruyama method.	23
Figure 2.8 : Impression norm of matrix M for daily volatility by Milstein method.	23
Figure 2.9 : Impression norm of matrix M for daily volatility by stochastic Runge-Kutta method.....	23
Figure 2.10 : BIST-100 between 02.01.2012 and 31.12.2012.....	23
Figure 3.1 : Distribution of logarithmic stock return when $r = 7.5\%$, $\kappa = 6$ and $\rho = 0.8$	31
Figure 3.2 : Distribution of logarithmic stock return when $r = 7.5\%$, $\kappa = 0.1$ and $\rho = -0.8$	31
Figure 3.3 : Mean Excess (left) and QQ (right) plots for positive correlation coefficient.....	33
Figure 3.4 : Mean Excess (left) and QQ (right) plots for negative correlation coefficient.....	34
Figure 3.5 : Hill plots for positive correlation coefficients.....	35
Figure 3.6 : Hill plots for negative correlation coefficients.....	36
Figure 3.7 : Distributions of logarithmic BIST-100 returns between 02.01.2004 and 17.06.2013.....	38
Figure 3.8 : ME (left) and QQ (right) plots of BIST-100 for the right tail, 2004 - 2013.	38
Figure 3.9 : Hill plot of BIST-100 for the right tail, 2004 - 2013.....	38
Figure 3.10 : Distributions of logarithmic BIST-100 (returns multiplied by -1) negative returns between 02.01.2004 and 17.06.2013.	39
Figure 3.11 : ME (left) and QQ (right) plots of BIST-100 for the left tail, 2004 - 2013.....	39
Figure 3.12 : Hill plot of BIST-100 for the left tail, 2004 - 2013.....	39

Figure 3.13: The average logarithmic stock return for $\xi = 0.1$ when the variance of the stock increases: (a) $v_0 = 0.2, \theta = 0.3$, (b) $v_0 = 0.3, \theta = 0.4$, and (c) $v_0 = 0.4, \theta = 0.5$	41
Figure 3.14: The average logarithmic stock return for $\xi = 0.1$ when the variance of the stock decreases: (a) $v_0 = 0.3, \theta = 0.2$, (b) $v_0 = 0.4, \theta = 0.3$, and (c) $v_0 = 0.5, \theta = 0.4$	41
Figure 3.15: Daily Interest Rates, 1996 - 2013.	42
Figure 3.16: Daily Interest Rates, 2010 - 2013.	43
Figure 3.17: Bist100 vs Interest Rates.....	43
Figure 4.1 : One path of MBS and MJD while $\lambda = 2$	47
Figure 4.2 : One thousand simulation paths of MBS (left) and MJD (right) while $\mu_X = 0$ and $\sigma_X = 1$ for MJD.	47
Figure 4.3 : Histograms of MBS (left) and MJD (right) with the best fitted normal distribution while $\mu_X = 0$ and $\sigma_X = 1$ for MJD.	47
Figure 4.4 : Solutions behavior of MJD while $\mu_X = -0.2$ and $\sigma_X = 1$	48
Figure 4.5 : Solutions behavior of MJD while $\mu_X = 0.2$ and $\sigma_X = 1$	49
Figure 4.6 : Solutions behavior of MJD while $\sigma_X = 0.22$ and $\mu_X = 0$	50
Figure 4.7 : Solutions behavior of MJD while $\sigma_X = 0.55$ and $\mu_X = 0$	51
Figure 4.8 : Extreme value analysis of the MBS model: ME-plot (top-left), QQ-plot (top-right) and Hill-plot (bottom).	54
Figure 4.9 : Impression Matrix Norms of the MBS model (top) and MJD for different means (bottom-left) and variances (bottom-right) of the jump.	55

BEHAVIORAL CLASSIFICATION OF STOCHASTIC DIFFERENTIAL EQUATIONS IN MATHEMATICAL FINANCE

SUMMARY

We study the behavior of solutions for stochastic differential equations such as Heston stochastic volatility model, Merton-Black Scholes model and Merton's Jump Diffusion model. We examine the numerical solutions using Euler Maruyama, Milstein and stochastic Runge-Kutta methods when we analyze Heston stochastic volatility model to investigate whether there is a role of the methods for different volatility cases or not, related to the impact of cumulative errors on this application. We perform simulations for different stock market conditions by using the large data set from Borsa Istanbul-100 (BIST-100).

We use volatilities in terms of extreme values at the overlapping case when we examine initial and long term volatilities for the application of the Heston model. While we explore strengths and limitations of Heston stochastic volatility model, Merton-Black Scholes model and Merton's Jump Diffusion model based on behavior of their numerical solutions, we suggest some model improvements in the light of the applications. Moreover, we introduce 3-dimensional matrix norms as generalizations of the matrix norms and prove the related lemmas, Duran and İzgi 2015, by using the applicable numerical linear algebra and analysis arguments. Furthermore, we define moving matrix for 2D and 3D matrices. Afterwards, we define market impression matrix norm as an application to the 3-dimensional matrix norms using moving matrices, Duran and İzgi, 2015. We can benefit from it to quantify market impression approximately by means of the numerical solutions for the stochastic differential equations. We analyze the simulation results for various parameters such that we perform high peak and fat-tail analysis for the impact of Heston, Merton-Black Scholes and Merton's jump diffusion models parameters' on the simulations of the extreme situations by using the first four standardized moments and extreme value tools such as quantile quantile (QQ), mean excess (ME) and Hill plots to examine the fat-tailness of the distributions. We also illustrate high peak and fat-tail analysis for BIST-100 index.

On the other hand, we investigate 3D dynamics of the average logarithmic stock return, interest rate and speed of mean reversion variables, together. In addition, we believe that polarization and the transitions between polarizations and comovements are important part of extreme situation picture. Therefore, we investigate comovement and polarization of interest rates and daily returns of BIST-100 index in order to understand the corresponding behavioral dynamics. Heston stochastic volatility model predicts that the average logarithmic stock return increases as interest rate rises. Actually, we observe that there are also sufficiently large time intervals where interest rates were decreased and stock prices increased gradually in US stock markets and Borsa Istanbul, unlike the Heston stochastic volatility model suggests.

Moreover, we analyze and compare the behavior of solutions for Merton-Black Scholes model and Merton's Jump Diffusion model. Especially, we focus on analyses of logarithmic stock price distributions obtained for these models using impression matrix norm and extreme value theory perspective. We achieved to present jump parameters' effects onto the behavior of solutions and also logarithmic stock price distributions using jump-adapted approximation method. Finally, we present price fluctuations for the Merton's jump diffusion and the Merton-Black Scholes models using impression matrix norm which reflects the effects of the jump parameters explicitly.

MATEMATİKSEL FİNANSTAKİ STOKASTİK DİFERANSİYEL DENKLEMLERİN DAVRANIŞSAL SINIFLANDIRMASI

ÖZET

Stokastik diferansiyel denklemlerden Heston stokastik volatilité, Merton-Black Scholes ve Merton sıçramalı difüzyon modellerinin çözümlerinin davranışları üzerine çalışılmıştır. Literatürde oldukça çok kullanılan Heston modeli 1993 yılında; Cox, Ingersoll ve Ross (CIR) tarafından faiz oranları için 1985 yılında yapılan CIR modelinden türetilmiştir. Her iki modelin uygulamalarında da sırasıyla varyans ve faiz oranlarının pozitifliği için Feller'in 1951 yılında yayınlanan makalesinde ortaya koyduğu Feller koşulunun dikkate alınması gerekmektedir.

Bir diğer model olan Merton-Black Scholes modeli ise Robert C. Merton tarafından 1960'ların sonu ve 1970'lerin başlarında geliştirilmiştir. İlk olarak ise Fisher Black ve Myron Scholes tarafından 1973 yılında yayınlanan makalelerinde kullanılmıştır. Bu model sayesinde 1997 yılında Ekonomi dalında Nobel ödülüne layık görülmüşlerdir. Ortaya konan difüzyon modeli her ne kadar yol gösterici olması açısından kullanışlı olsa da, literatürdeki uygulama sonuçlarından da görülebileceği gibi piyasalardaki ani fiyat değişimlerini yansıtmakta yeterli değildi. Bu yüzden Merton 1976 yılında Merton-Black Scholes modelini geliştirerek hisse senedi fiyatlarındaki sıçrama durumlarını da yansıtan Merton sıçramalı difüzyon modelini elde etmiştir.

Bu modellerin bazı parametrelerinin çözümlere olan etkileri ele alınan yöntemler yardımıyla ayrıntılı olarak incelenmiştir. Simülasyon uygulamalarından değişik volatilité durumlarında, simülasyon yöntemlerinin birikimli hatalarından kaynaklanan etkilerinin olup olmadığını araştırmak için Heston stokastik volatilité modeli Euler-Maruyama, Milstein ve Stokastik Runge-Kutta metodlarıyla analiz edilmiştir. Hisse senedi piyasalarının değişik koşulları için Borsa İstanbul - 100 (BIST - 100) endeksinin dataları kullanılarak simülasyonlar yapılmıştır. Yapılan simülasyonlardan elde edilen sonuçlar gerçek datalarla karşılaştırılarak analiz edilmiştir.

Heston stokastik volatilité modelinin uygulamasında başlangıç ve uzun vadeli volatiliteleri elde etmek için üst üste gelme durumlarındaki ekstremum değerler yöntemi kullanılmıştır. Ekstremum değerler yöntemiyle yaklaşık olarak elde edilen günlük volatiliteler de kullanılarak modelin avantajları ve limitleri araştırılmıştır. Ayrıca, matris normlarının genellemeleri olarak 3-boyutlu matrisler için norm tanımlamaları ve ilgili lemmaların da ispatları, Duran ve İzgi 2015, uygun nümerik lineer cebir ve analiz argümanları kullanılarak yapılmıştır. Daha sonra, 2-boyutlu ve 3-boyutlu hareketli matris tanımlamaları yapılmış olup, tanımlanan 3-boyutlu matris normlarının uygulaması olarak da piyasanın izlenim matris normu, hareketli matrisler üzerinde tanımlanmıştır, Duran ve İzgi, 2015. Bu normların gerek simülasyon gerekse gerçek datalarla yapılan uygulamaları ayrıntılı ve karşılaştırmalı olarak ele alınmıştır. Yapılan analizler ve incelemeler ışığı altında izlenim matris normunun kullanışlılığı da ortaya konulmuştur.

Birçok disiplin dallarında ekstremum durumları anlamak ve olasılıklarının tahmininde bulunmak için ekstremum değer teorisi oldukça önemli rol üstlenmektedir. Finans, ekonomi, yer bilimi ve hidroloji gibi alanlar da bu teorinin uygulama alanlarından bazılarıdır. Finansal anlamda, ekstremum durumlar kayıp veya kazançların oldukça yüksek olabileceği durumlar olmasından dolayı, dikkate alınması ve incelenmesi gereken önemli noktalardan biridir. Bu yüzden Heston, Merton-Black Scholes ve Merton sıçramalı difüzyon modellerinin bazı parametrelerinin simülasyon sonuçlarındaki ekstremum durumlarına olan etkilerini incelemek için, uç nokta ve kalın kuyruk analizleri standartlaştırılmış ilk dört moment değerleri ve ekstremum değer teorisi araçlarından quantile quantile, ortalamayı aşan (mean excess) ve tepe (hill) grafikleri yardımıyla yapılmıştır.

Bu metodlar kullanılarak BIST-100 endeksi için de uç nokta ve kalın kuyruk analizleri örneklendirilmiştir. Böylece gerçek dataların ekstremum durumlarındaki davranışları ile gerçek datalar kullanılarak elde edilen simülasyon sonuçlarındaki ekstremum durumlar karşılaştırılmıştır.

Finans piyasaları dinamik olduğundan birden çok parametrenin birbirlerine göre etkilerini ve davranışlarını incelemek oldukça önemlidir. Bu yüzden modelleme ve simülasyonlar yapılırken ele alınan model parametrelerinin dinamiklerini kontrol altında tutmak zor ve gerekli işlemlerdir. Bu sebepten ötürü Heston stokastik volatilité modeli ile yapılan simülasyonlarda; logaritmik hisse senedi getirisi, faiz oranı ve ortalamaya dönüş hızı dinamikleri 3-boyutlu olarak araştırılmıştır. Bu dinamiklerin birbirlerine olan etkileri 3-boyutlu grafikler yardımıyla da değişik market senaryoları için kapsamlı bir şekilde ayrı ayrı olarak ortaya konulmuştur.

Ayrıca, dinamiklerdeki eş hareketlilik ve eş hareketlilikten zıt hareketliliğe geçişin ekstremum durumlarda önemli olduğuna inanılmaktadır. Bu yüzden, faiz oranı ve günlük BIST-100 endeks dinamiklerinin davranışlarını daha iyi anlamak için eş ve zıt hareketleri incelenmiştir. Heston modeli logaritmik hisse senedi getirisinin, faiz oranlarının artışına paralel olarak artacağını öngörmektedir. Aslında, Heston modelinin aksine yeterince geniş bir zaman aralığında faiz oranlarının düşerken gerek Amerikan hisse senedi piyasasının gerekse Borsa İstanbul endekslerinin arttığı gözlemlenmiştir.

Bunun yanı sıra, gerçek piyasalarda karşımıza çıkan sıçrama durumlarını anlamak ve kontrol altında tutmak da yatırım stratejisi ve risk kontrolü için oldukça önemli ve gereklidir. Bu yüzden, Merton-Black Scholes modeli ile Merton sıçramalı difüzyon modelinin çözüm davranışları analiz edilerek, elde edilen sonuçlar karşılaştırılmıştır. Özellikle, simülasyonlardan elde edilen logaritmik hisse senedi fiyat dağılımları incelenmiş olup, ilgili dağılımlar izlenim matris normu ve ekstremum değer teorisi kullanılarak analiz edilmiştir. Model parametrelerinin, sıçramalı stokastik diferansiyel denklemlerin sayısal çözüm yöntemlerinden olan sıçrama uyumlu (jump-adapted) metodla elde edilen logaritmik hisse senedi fiyat dağılımına ve modellerin çözüm davranışlarına olan etkisi gösterilmiştir.

İlgili analizler dahilinde Merton sıçramalı difüzyon modelinin Merton-Black Scholes modeline göre fiyatlardaki ekstremum durumlarını daha iyi yansıttığı gözlemlenmiştir. Merton sıçramalı difüzyon modelinin bu önemli özelliği dikkate alındığı takdirde yatırım stratejisi belirlenme aşamasında önemli olacağı kanaatine varılmıştır.

Son olarak, Merton-Black Scholes modeli ile Merton sıçramalı difüzyon modelinin fiyat salınımları, sıçrama parametrelerinin etkilerini de yansıtan izlenim matris norm kullanılarak açık bir şekilde gösterilmiştir. İzlenim matris normunun simülasyon veya gerçek datalarla yapılan analizlerde sıçramaların varlığının belirlenmesinde alternatif bir araç olarak kullanılabilceği sonucu elde edilmiştir. Ayrıca izlenim matris normunun, sıçrama potansiyelinin olduğu tam olmayan marketlerdeki gerçek hisse senedi piyasalarında da hisse senedi fiyat salınımlarını ve davranışlarını anlamak için kullanışlı olacağı sonucuna varılmıştır.

1. INTRODUCTION

We study several behaviors of stochastic differential equations (SDEs) in Mathematical Finance. The solution space of stochastic differential equations has rich behaviors. Also, the solution space of SDEs in mathematical finance has certain characteristics such as overreaction, underreaction, jumps, stable and unstable situations (see Duran and Caginalp [1], Duran [2] and references therein). In particular, we focus on advantages and limitations of solutions for Heston Stochastic Volatility model [3], Merton-Black Scholes model [4] and Merton's Jump Diffusion model [5] among others. In addition, we analyze these models with respect to the extreme value theory and impression matrix norm in order to understand extreme behaviors of the models and model parameters' effects onto the impression of the market while we perform simulations for the real data (see Duran and İzgi [6–8]). Moreover, we discuss financial interpretation of the analysis results and compare them by the sense of financial usefulness. In this chapter, we present basic definitions, theorems, numerical methods and some of the properties of the SDEs which we generally use throughout the thesis.

1.1 Basic Stochastic Differential Equations

In mathematics, Brownian motion is described by the Wiener process. Although it originates in work of botanist Robert Brown in 1828, a continuous-time stochastic process named in honor of Norbert Wiener who was first proved it mathematically in 1923. It is one of the best known Lévy processes (stochastic processes, which is right continuous with left limit, by the stationary independent increments) and occurs frequently in pure and applied mathematics, economics and physics among others [9].

Definition 1.1.1. (Brownian motion) A standard one-dimensional Brownian motion is a continuous, adapted process $W = \{W_t, \mathcal{F}_t; 0 \leq t \leq \infty\}$, defined on some probability space $(\Omega, \mathbf{F}, \mathbb{P})$, with the properties that $W_0 = 0$ a.s. and for $0 \leq s < t$, the increment $W_t - W_s$ is independent of \mathbf{F}_s and is normally distributed with mean zero and variance $t - s$.

Properties of Brownian Motion

- $W(0) = 0$.
- $W(t) - W(s)$ is normally distributed with mean zero and variance $t - s$, for $s < t$.
- The process W has independent increments: for any set of times $0 \leq t_1 < t_2 < \dots < t_n$, the random variable $W(t_2) - W(t_1)$, $W(t_3) - W(t_2)$, ..., $W(t_n) - W(t_{n-1})$ are independent.
- The sample paths $\{W(t); t \geq 0\}$ are continuous functions of t . Moreover, the paths of Brownian motion are very erratic and they are nowhere differentiable.
- $E[W_t^4] = 3t^2$ and $E[|W_t - W_s|^4] = 3|t - s|^2$. More generally;

$$E[W_t^{2k}] = \frac{(2k)!}{2^k \cdot k!} t^k \text{ and } E[W_t^{2k+1}] = 0, \quad k \in \mathbb{Z}_+.$$

- Brownian motion is a martingale such that $E[W_t | \mathbf{F}_s] = W_s$. (for more details [9, 10]).

Itô's formula (or Itô lemma) is the analog in Stochastic calculus of the chain rule in classical calculus. It is quite useful in Stochastic Calculus, as it is use to find SDEs satisfied by functions of a particular class of stochastic processes. It has very wide applications at the mathematical finance.

Theorem 1.1.1. (Itô's formula) Let $f(t, x)$ be a function that has a continuous derivative with respect to t and two continuous derivatives with respect to x (i.e. $f \in \mathbb{C}^{1,2}$). Then, the process $f(t, X(t))$ satisfies

$$df(t, X(t)) = \left[f_t + \frac{1}{2} \sigma^2 f_{xx} \right] (t, X(t)) dt + f_x(t, X(t)) dX(t)$$

for the given diffusion process

$$dX(t) = \mu(t, X(t)) dt + \sigma(t, X(t)) dW(t).$$

If we substitute for $dX(t)$, we get the following useful form of Itô's rule:

$$df(t, X(t)) = \left[f_t + \mu f_x + \frac{1}{2} \sigma^2 f_{xx} \right] (t, X(t)) dt + (\sigma f_x)(t, X(t)) dW(t).$$

1.1.1 Merton-Black Scholes model

Merton-Black Scholes (MBS) model is one of the most important mathematical model in the finance literature. Robert C. Merton developed the finance theory of this model in the late of 1960 and early 1970s. Fisher Black and Myron Scholes was used this model at their paper in 1973 [4] and it was the first paper published by using this model. After that, Merton and Scholes received Nobel Price in Economics in 1997 for their pioneer work. Unfortunately, Black could not get the Nobel Price since he passed away in 1995.

Merton-Black Scholes model has the following general form:

$$dS(t) = S(t)\mu dt + S(t)\sigma dW(t) \quad (1.1)$$

where μ is linear drift coefficient, σ is linear diffusion coefficient and $W(t)$ is a standard one-dimensional Brownian motion. Moreover, it can be shown that $S(t) = S(0)e^{(\mu - \frac{1}{2}\sigma^2)t + \sigma W(t)}$, $S(0) = s(0)$ is the solution of (1.1) by using the Itô's formula [11]. MBS model predicts that the stock price can only change by a small amount in a short interval of time.

1.1.2 Merton's jump diffusion model

Merton was the one of the first scientist who achieved to introduce and analyze jump and diffusion process by using rich behavior of the solution space of stochastic differential equations at his model. In 1976, Merton extended the MBS diffusion model to a model that also has a jump component. Merton take MBS model one step a head with his jump-diffusion model which allows for a positive probability of a stock price change of extraordinary magnitude in a short or long interval of time [see figure 4.2 and [5]]. He suggested the number of the jumps $N(t)$ between time 0 and time t should be a so-called Poisson process which governed by poisson distribution.

Merton's jump-diffusion (MJD) model can be represented with the following SDE:

$$dS(t) = S(t-)\mu dt + S(t-)\sigma dW(t) + S(t-)dJ(t) \quad (1.2)$$

where μ and σ are constant, W is a standard one-dimensional Brownian motion, $S(t-)$ is a value of just before a potential jump, and J is a jump process independent of W

with piecewise constant sample paths. In particular, J (compound poisson process) is given by

$$J(t) = \sum_{j=1}^{N(t)} (X_j - 1) \quad (1.3)$$

where X_1, X_2, \dots are identical independent random variables and independent of $N(t)$ (as well as W). Here, $N(t)$ is a counting process such that there are random arrival times $0 < \tau_1 < \tau_2 < \dots$ and $N(t) = \sup\{n : \tau_n \leq t\}$ [12]. The size of jump is $X_j - 1$ if $t = \tau_j$ and 0 if t does not coincide with any of the τ_j . We can also interpret the Merton's jump-diffusion model such that the increment in S at t depends on $S(t-)$ and not $S(t)$. The jump in S at time t is $S(t) - S(t-)$ and it is 0 unless the J jump times. At the jump time ($t = \tau_j$),

$$S(\tau_j) = S(\tau_j-)X_j.$$

It means that the X_j 's are just the ratio of the asset price before and after a jump. On the other hand, the solution of (1.2) is given by

$$S(t) = S(0)e^{(\mu - \frac{1}{2}\sigma^2)t + \sigma W(t)} \prod_{j=1}^{N(t)} X_j \quad (1.4)$$

that is nothing more than generalization of the corresponding solution for geometric Brownian motion in (1.1). It can be shown that (1.4) is the solution of the (1.2) by using Itô-Doebelin formula for jump process.

1.1.3 Heston stochastic volatility model

In Heston's stochastic volatility model the asset price process S_t and the variance process $v_t := \sigma_t^2$ solve the following two-dimensional stochastic differential equation [3]:

$$\begin{aligned} dS_t &= (r - q)S_t dt + \sqrt{v_t}S_t dW_1(t) \\ dv_t &= \kappa(\theta - v_t)dt + \xi\sqrt{v_t}dW_2(t) \end{aligned}$$

At the Merton-Black-Scholes model [4] the volatility σ was assumed to be constant. The main difference between MBS and Heston model is volatility behavior. It is stochastic and it satisfies mean reverting property with a mean reverting drift at the Heston model. The W_1 and W_2 represent Brownian motions of asset price process and the variance process are correlated, with correlation coefficient $\rho \in [-1, 1]$. We also

use the following SDE for the related correlation:

$$dW_2 = \rho dW_1 + \sqrt{1 - \rho^2} dW, \quad \rho \in [-1, 1].$$

On the other hand, $\xi > 0$ is the volatility parameter of the variance process, $r \geq 0$ is the risk-free interest rate, $q \geq 0$ is the dividend yield, $\kappa > 0$ is the rate of mean reversion, and $\theta > 0$ is the long run variance level [3]. Stochastic volatility model of Heston (1993) is frequently used. Heston's model is derived from the CIR model of Cox, Ingersoll and Ross (1985) for interest rates [13]. We choose the parameters as they satisfy the Feller condition $2\kappa\theta \geq \xi^2$ at our simulations so that non-negativity of volatility can be guaranteed [14].

1.2 Numerical Methods

Definition 1.2.1. The discrete time approximation is said to converge weakly with order p to y if for each polynomial g (which is $2(p + 1)$ times continuously differentiable), $\exists C > 0$ (independent of h) and $\delta > 0$ such that

$$\|E(g(\bar{y}_N)) - E(g(y(t_N)))\| \leq Ch^p, \quad h \in (0, \delta).$$

Definition 1.2.2. Let \bar{y}_N be the numerical approximation to $y(t_N)$ after N steps with constant stepsize $h = (t_N - t_0)/N$; then \bar{y} is said to converge strongly to y with order p if $\exists C > 0$ (independent of h) and $\delta > 0$ such that

$$E(\|\bar{y}_N - y(t_N)\|) \leq Ch^p, \quad h \in (0, \delta).$$

1.2.1 Euler Maruyama method

Lets consider the following SDEs:

$$dy = f(t, y)dt + g(t, y)dW, \quad y(0) = y_0. \quad (1.5)$$

The first method for solving SDEs numerically was Euler-Maruyama method [15]. If we apply this method to the (1.5), Euler-Maruyama method has form as follow :

$$\Delta y_i = f(t_i, y_i)\Delta t_i + g(t_i, y_i)\Delta W_i$$

$$\Delta t_i = t_{i+1} - t_i$$

$$\Delta W_i = W_{i+1} - W_i$$

The Euler-Maruyama method for SDEs has strong order 1/2. Also Brownian motion ΔW_i can be modeled as $\Delta W_i = z_i \sqrt{\Delta t_i}$ where z_i is chosen from $N(0,1)$ standard normally random variable, as well.

1.2.2 Milstein method

Milstein method has the following form for the equation (1.5):

$$\begin{aligned}\Delta y_i &= f(t_i, y_i) \Delta t_i + g(t_i, y_i) \Delta W_i + \frac{1}{2} g(t_i, y_i) \frac{\partial g}{\partial y}(t_i, y_i) (\Delta W_i^2 - \Delta t_i) \\ \Delta t_i &= t_{i+1} - t_i \\ \Delta W_i &= W_{i+1} - W_i\end{aligned}$$

The Milstein Method has strong order 1 for solving SDEs [16]. It is obvious from the above equation if the (1.5) does not have y term in the diffusion part $g(t, y)$, Milstein Method is identical to the Euler Maruyama Method.

1.2.3 Stochastic Runge-Kutta method

When we consider the $dy = f(t, y)dt + g(t, y)dW$ SDEs, maybe the most general class of Stochastic Runge-Kutta (SRK) methods takes the form:

$$\begin{aligned}Y_i &= y_n + h \sum_{j=1}^{i-1} a_{ij} f(Y_j) + J_1 \sum_{j=1}^{i-1} b_{ij}^{(1)} g(Y_j), \quad i = 1, \dots, s \\ y_{n+1} &= y_n + h \sum_{j=1}^s \alpha_j f(Y_j) + J_1 \sum_{j=1}^s \gamma_j g(Y_j)\end{aligned}$$

At the above equations, $A = (a_{ij})$ and $B = (b_{ij})$ are matrices in $\mathbb{R}^{s \times s}$ while $\alpha^T = (\alpha_1, \dots, \alpha_s)$ and $\gamma^T = (\gamma_1, \dots, \gamma_s)$ are row vectors in \mathbb{R}^s . If both A and B are strictly lower triangular matrices then method is said to be explicit, otherwise it is implicit. At this method, the stochastic component comes from the J_1 Stratonovich integral ($J_1 = \int_{t_n}^{t_{n+1}} \circ dW$) associated with B and γ [17].

An explicit stochastic Runge-Kutta method with strong order 2

The SRKs method with strong order 2 can be written as

$$\begin{aligned}Y_i &= y_n + h \sum_{j=1}^{i-1} a_{ij} f(Y_j) + \sum_{j=1}^{i-1} (b_{ij}^{(1)} J_1 + b_{ij}^{(2)} \frac{J_{10}}{h}) g(Y_j), \quad i = 1, \dots, s \\ y_{n+1} &= y_n + h \sum_{j=1}^s \alpha_j f(Y_j) + \sum_{j=1}^s (\gamma_j^{(1)} J_1 + \gamma_j^{(2)} \frac{J_{10}}{h}) g(Y_j)\end{aligned}$$

The maximum strong order of the stochastic Runge-Kutta method is 1.0 when the method does not include J_{10} (i.e. $J_{10} = \int \int \circ dW_{s_1} ds$). On the other hand, J_1 and J_{10} can be defined as $J_1 = g_1 \sqrt{h}$ and $J_{10} = h^{3/2}(g_1 + g_2/\sqrt{3})/2$ for a given pair (g_1, g_2) of standard normally distributed random variables (see [17–20] and references therein).

1.3 Stochastic Calculus for Jump Process

We present the Itô's formula for the continuous process, which is the analog in Stochastic calculus of the chain rule in classical calculus, at the previous section. The main question is "how can we describe the time evolution of the process while the processes does not continuous? or the processes have jumps term?". The new version of the Itô's formula is needed to overcome the difficult situations.

1.3.1 Itô-Doebelin formula for jump process

Theorem 1.3.1. *Let X be a diffusion process with jumps, defined as the sum of a drift term, a Brownian stochastic integral and a Poisson process:*

$$dX(t) = \mu(t, X(t))dt + \sigma(t, X(t))dW(t) + dJ(t)$$

or in the integral form

$$X(t) = X(0) + \int_0^t \mu(s, X(s))ds + \int_0^t \sigma(s, X(s))dW(s) + \sum_{i=1}^{N_t} \Delta J_i(t)$$

where $\mu(t, X(t))$ and $\sigma(t, X(t))$ are continuous adapted process with $E[\int_0^T \sigma^2 dt] < \infty$. Then, for any function $f : [0, T] \times \mathbb{R} \rightarrow \mathbb{R}$, $f \in \mathbb{C}^{1,2}$, the process $f(t, X(t))$ can be represented as follow:

$$\begin{aligned} f(t, X(t)) &= f(0, X(0)) + \int_0^t \left(\frac{\partial f}{\partial s} + \mu \frac{\partial f}{\partial x} + \frac{1}{2} \sigma^2 \frac{\partial^2 f}{\partial x^2} \right) (s, X(s)) ds \\ &+ \int_0^t \left(\sigma \frac{\partial f}{\partial x} \right) (s, X(s)) dW(s) + \sum_{0 < s \leq t} [f(s, X(s)) - f(s-, X(s-))] \end{aligned} \quad (1.6)$$

The differential form of the Itô-Doebelin formula for jump process (1.6) is not always possible since it is not always possible to write the sum of the jumps in differential form. Shreve explains this situation at his book more explicitly [21]. Under the given information, if we assume that the last term of the Itô-Doebelin formula can be written

in differential form then we can rewrite (1.6) in differential form as follow:

$$df(t, X(t)) = \underbrace{\left(\frac{\partial f}{\partial t} + \mu \frac{\partial f}{\partial x} + \frac{1}{2} \sigma^2 \frac{\partial^2 f}{\partial x^2} \right)(t, X(t)) dt + \left(\sigma \frac{\partial f}{\partial x} \right)(t, X(t)) dW(t)}_{\text{It\^o's formula for the continuous process}} + \underbrace{[f(t, X(t)) - f(t-, X(t-))] dN(t)}_{\text{characterizes the jumps}} \quad (1.7)$$

It\^o-Doeblin formula for jump process

Example 1.3.1. (Geometric Poisson process, [Shreve, [21]]) Let's consider the geometric Poisson process

$$S(t) = S(0) \exp\{N(t) \log(\sigma + 1) - \lambda \sigma t\} = S(0) e^{-\lambda \sigma t} (\sigma + 1)^{N(t)}, \quad (1.8)$$

where $\sigma > -1$ is a constant. If $\sigma > 0$, this process jumps up and moves down between jumps; if $-1 < \sigma < 0$, it jumps down and moves up between jumps. Moreover, we can write $S(t) = S(0) f(X(t))$, where $f(x) = e^x$ and $X(t) = N(t) \log(\sigma + 1) - \lambda \sigma t$ where the continuous part is $X^c(t) = -\lambda \sigma t$ and pure jump part is $J(t) = N(t) \log(\sigma + 1)$. Now, we can use It\^o-Doeblin formula for jump processes,

$$\begin{aligned} S(t) &= S(0) \left(f(X(0)) - \lambda \sigma \int_0^t f'(X(u)) du + \sum_{0 < u \leq t} [f(X(u)) - f(X(u-))] \right) \\ &= S(0) - \lambda \sigma \int_0^t S(u) du + \sum_{0 < u \leq t} [S(u) - S(u-)] \end{aligned} \quad (1.9)$$

If there is a jump at time u , then $S(u) = (\sigma + 1)S(u-)$, then

$$S(u) - S(u-) = \begin{cases} \sigma S(u-), & \text{whenever there is a jump at time } u; \\ 0, & \text{if there is no jump at time } u. \end{cases} = \sigma S(u-) \Delta N(u).$$

This representation permits us to rewrite the sum on the right-hand side in a integral form as follow:

$$\sum_{0 < u \leq t} [S(u) - S(u-)] = \sum_{0 < u \leq t} \sigma S(u-) \Delta N(u) \approx \sigma \int_0^t S(u-) dN(u).$$

It does not matter whether we write the Riemann integral on the right-hand side of (1.9) as $\int_0^t S(u) du$ or $\int_0^t S(u-) du$. The integrand in these two integrals differ at only finitely many times. When we integrate with respect to du , these differences do not matter since the measure of these difference cases are zero. Therefore, we may rewrite (1.9) as

$$\begin{aligned} S(t) &= S(0) - \lambda \sigma \int_0^t S(u-) du + \sigma \int_0^t S(u-) dN(u) \\ &= S(0) + \sigma \int_0^t S(u-) dCN(u) \end{aligned}$$

where CN is the compensated Poisson process $CN(u) = N(u) - \lambda u$, which is a martingale. In this case, the Itô-Doebelin formula (1.9) has a differential form (for more details please see [21–23]), namely,

$$dS(t) = \sigma S(t-)dCN(t) = -\lambda \sigma S(t)dt + \sigma S(t-)dN(t).$$

We were able to obtain this differential form since we were able to write $f(X(u))$ (i.e. jump in $S(u)$) at the jump time u in terms of $f(X(u-))$ (i.e. in terms of $S(u-)$ before the jump time).

1.3.2 Simulation strategy of the jump process

Simulation of the jump diffusion process is harder than simulation of the pure diffusion process. Therefore, strategy of the simulation takes important role for the jump diffusion model at the numerical approach. Although it is hard to distinguish effects of the jump and diffusion terms at the model, simulation of the process at a fixed set of dates is one of the strategy using at the literature. On the other hand, simulation of the jump diffusion model can be done by simulating the jump times τ_1, τ_2, \dots explicitly. At the latter strategy, effects of the jumps are presented more clearly. Moreover, combination of these strategies, which is also called as jump-adapted approximations, can be used at the simulation of the jump diffusion process (for more details please see [12, 23]).

Simulation at fixed dates

We can generalize explicit solution of the Merton's jump diffusion model in (1.4) at time t_1, t_2, \dots, t_n as follow:

$$S(t_{i+1}) = S(t_i)e^{(\mu - \frac{\sigma^2}{2})(t_{i+1} - t_i) + \sigma[W(t_{i+1}) - W(t_i)]} \prod_{j=N(t_i)+1}^{N(t_{i+1})} X_j. \quad (1.10)$$

Now, we can simulate directly from this representation or we can use its equivalent representation which obtains under the $Y(t) = \log(S(t))$ change of variable. If we do so, the explicit solution in (1.10) become as follow by changing the products with sums which is preferable at the simulations

$$Y(t_{i+1}) = Y(t_i) + (\mu - \frac{\sigma^2}{2})(t_{i+1} - t_i) + \sigma[W(t_{i+1}) - W(t_i)] + \sum_{j=N(t_i)+1}^{N(t_{i+1})} \log(X_j). \quad (1.11)$$

If we use this representation while we perform the simulations, we can generate samples of the $S(t_i)$ by exponentiate simulated values of the $X(t_i)$. The following steps can be used for simulating (1.11) from t_i to t_{i+1} :

1. generate standard normal random variable: $Z \sim \mathbb{N}(0, 1)$
2. generate N poisson process: $N \sim \text{Poisson}(\lambda(t_{i+1} - t_i))$; if $N = 0$, set $M = 0$ and go to step 4
3. generate $\log(X_1), \dots, \log(X_N)$ from their common distribution and set $M = \log(X_1) + \dots + \log(X_N)$
4. lastly, set

$$Y(t_{i+1}) = Y(t_i) + \left(\mu - \frac{\sigma^2}{2}\right)(t_{i+1} - t_i) + \sigma\sqrt{t_{i+1} - t_i}Z + M.$$

We take account two main properties of the Poisson process at this method: the increment $N(t_{i+1}) - N(t_i)$ has a Poisson distribution with mean $\lambda(t_{i+1} - t_i)$, and it is independent of increments of N over $[0, t_i]$. We can simplify this method with assumptions on the distribution of the X_j (i.i.d.). If we assume X_j have lognormal distribution $\mathbb{LN}(a, b^2)$, then $\log(X_j) \sim \mathbb{N}(a, b^2)$ and

$$\sum_{j=1}^n \log(X_j) \sim \mathbb{N}(an, b^2n) = an + b\sqrt{n}\mathbb{N}(0, 1).$$

Now, we can replace step 3 with "generate new standard normal random variable: $Z_2 \sim \mathbb{N}(0, 1)$; set $M = aN + b\sqrt{N}Z_2$ " [12].

Simulating jump times

Simulation method based on fixed dates for the equation (1.11) generates the total number of jumps in each time interval $(t_i, t_{i+1}]$ by using the fact that the number of jumps has a Poisson distribution. It is the disadvantage part of the this method. Therefore, simulating jump times is an alternative method based on simulates the jump times τ_1, τ_2, \dots explicitly. Simulation of the (1.2) reflects jumps behavior at each jump time as in the real market by using the simulating jump times method, and it gets solution behavior analysis more easy and realistic.

$S(t)$ evolves like an ordinary Brownian motion between the two jump times since we have assumed that W and J in (1.2) are independent of each other. According to the

times τ_1, τ_2, \dots of the jumps,

$$S(\tau_{j+1}-) = S(\tau_j) e^{(\mu - \frac{\sigma^2}{2})(\tau_{j+1} - \tau_j) + \sigma[W(\tau_{j+1}) - W(\tau_j)]} \quad (\text{before the jump})$$

and

$$S(\tau_{j+1}) = S(\tau_{j+1}-) X_{j+1} \quad (\text{jump effects})$$

If we take logarithms and combining these steps, we get;

$$Y(\tau_{j+1}-) = Y(\tau_j) + (\mu - \frac{\sigma^2}{2})(\tau_{j+1} - \tau_j) + \sigma[W(\tau_{j+1}) - W(\tau_j)] + \log(X_{j+1}).$$

Finally, a general scheme for simulating one step of this recursion has the following form:

1. generate R_{j+1} from the exponential distribution with mean $1/\lambda$: $R_{j+1} = -\log(U)/\lambda$ with $U \sim \text{Unif}[0, 1]$.
2. generate standard normal random variable: $Z_{j+1} \sim \mathbb{N}(0, 1)$
3. generate the jump size $\log(X_{j+1})$
4. set $\tau_{j+1} = \tau_j + R_{j+1}$ and

$$Y(\tau_{j+1}-) = Y(\tau_j) + (\mu - \frac{\sigma^2}{2})R_{j+1} + \sigma\sqrt{R_{j+1}}Z_{j+1} + \log(X_{j+1}).$$

On the other hand, the two approaches to simulating $S(t)$ can be combined which is called as jump-adapted approximation. For instance, suppose we fix a date t in advance that we would like to include among the simulated dates. Suppose it happens that $\tau_j < t < \tau_{j+1}$ (i.e., $N(t) = N(t-) = j$). Then,

$$S(t) = S(\tau_j) e^{(\mu - \frac{\sigma^2}{2})(t - \tau_j) + \sigma[W(t) - W(\tau_j)]}$$

and

$$S(\tau_{j+1}) = S(t) e^{(\mu - \frac{\sigma^2}{2})(\tau_{j+1} - t) + \sigma[W(\tau_{j+1}) - W(t)]} X_{j+1}$$

[12].

The remainder of the thesis is organized as follows. In Chapter 2, we generally study the behavior of solutions for Heston stochastic volatility model on its real data applications. First of all, we introduce 3-dimensional matrix norms as generalizations

of the matrix norms and prove the related lemmas [6], by using the applicable numerical linear algebra and analysis arguments (see [24, 25] and references therein) and give the definition of the moving matrix [6]. Furthermore, we define market impression matrix norm as an application to the 3-dimensional matrix norms using moving matrix [6]. We focus on the numerical solutions and their comparisons using Euler Maruyama, Milstein and stochastic Runge-Kutta methods. Especially, we use these methods to investigate whether there is a role of the methods for different volatility cases or not, related to the impact of cumulative errors on this application. We use volatilities in terms of extreme values at the overlapping case when we examine initial and long term volatilities for the real data applications of the Heston model. At the end of this chapter, we analyze the simulation results for various parameters.

In Chapter 3, we briefly introduce the extreme value theory and its tools such as quantile quantile (QQ), mean excess (ME) and Hill plots. We present high peak and fat tail formation of logarithmic stock return distributions from Heston model under different market situations [7]. After that, we investigate fat-tail and high peak situations of the BIST-100 index between 02.01.2004 and 17.06.2013. Moreover, we examine 3D dynamics of the average logarithmic stock return, interest rate and speed of mean reversion variables [7]. Finally, we discuss the comovement and polarization of interest rates and daily returns of BIST - 100 index between 2010 and 2013.

In Chapter 4, we work on behavioral analysis of Merton-Black Scholes and Merton's Jump Diffusion Models [8]. Moreover, we present high peak and fat tail formation of logarithmic stock price distributions from Merton-Black Scholes and Merton's Jump Diffusion models for different model parameters using extreme value theory. We investigate and illustrate jump parameters effects onto the logarithmic stock price distribution for these models by the sense of impression matrix norm [8]. Chapter 5 concludes the thesis.

2. APPLICATION OF HESTON MODEL FOR BORSA ISTANBUL

Our goal in this chapter is to study the behavior of solutions for stochastic differential equations (SDEs) such as Heston model [3]. Heston model is a very useful stochastic volatility model used in financial markets where the evolution for the stock price volatility is described and the volatility is a random process. Market situations at relatively low volatility levels have attracted academic attention. For example, Duran and Bommarito [26] argued that there may be a temporary silence at the beginning of a credit crunch, especially when prices are overvalued at a high level, and the low market volatility may indicate the silence before a storm. We extend our approach [27] by using several numerical solution methods for Heston stochastic volatility model and by applying to Borsa Istanbul-100's (BIST-100) large data set between 04.01.2007 and 31.12.2012. Moreover, Duran and İzgi consider application of the Heston model for Borsa Istanbul using impression matrix norm at their paper [6]. Especially, we use Euler Maruyama, Milstein and stochastic Runge-Kutta (SRK) methods whose rates of convergence for the stochastic differential equations are 0.5, 1 and 2, respectively, [15–19]. We examine the trade-off between cost and robustness of the methods while choosing a suitable method for the application dealing with the relatively low volatility cases. We perform simulations for different stock market conditions by using the real large data set.

At the application of the Heston model, we also need to know the initial and long term variances like the other parameters. However, it can sometimes be hard to estimate these values for a large data set. For this purpose, the natural log ratio of the highest price to the lowest price [28], standard deviation or simple return based on the highest and the lowest prices in the interval can be considered by taking their squares. We prefer volatilities having simple return of extreme values at the overlapping case which is applied for closed-end funds [29] when we examine initial and long term volatilities of BIST-100 index for each year between 2007 and 2012. We also employ unit volatility of extreme values to estimate the volatilities of BIST-100 index in our analyses. It is important to find a method to quantify market impression

approximately, and summarize large data set in presence of several variables together. Although market price reflects all past publicly available information according to weak-form efficient-market hypothesis (EMH) [30], many traders believe that prices can be overvalued or undervalued. Therefore, we seek to find a scheme for market impression in addition to market price [6]. We believe that market impression may be expressed via several variables such as volatility, interest rate, and time, together.

2.1 3-Dimensional Matrix Norms

Matrix norms are essential parts of numerical linear algebra [24] and its applications in science, engineering and finance [6].

Definition 2.1.1. A 3-dimensional matrix norm $\| \cdot \|$ is a function from m -by- n -by- s complex matrices into \mathfrak{R} that satisfies the following properties:

- $\| A \| \geq 0$ and $\| A \| = 0$ if and only if $A = 0$;
- $\| \alpha A \| = |\alpha| \| A \|$, for scalar α ;
- $\| A + B \| \leq \| A \| + \| B \|$; where A and B are matrices in m -by- n -by- s dimensional space.

Definition 2.1.2. The 1 – norm and ∞ – norm of $A \in \mathbb{C}^{m \times n \times s}$ are defined as follows:

$$\| A \|_1 = \max_j \sum_{k=1}^s \sum_{i=1}^m | a_{ij}^{(k)} | = \text{the largest absolute block-column sum.}$$

$$\| A \|_\infty = \max_i \sum_{k=1}^s \sum_{j=1}^n | a_{ij}^{(k)} | = \text{the largest absolute block-row sum.}$$

Lemma 2.1.1. Let $A \in \mathbb{C}^{m \times n \times s}$ then the $\| A \|_1$ and $\| A \|_\infty$ are norms.

Proof. Proofs are straightforward and just come from the definition of them. □

Definition 2.1.3. The p – norm of $A \in \mathbb{C}^{m \times n \times s}$ is defined as follow:

$$\| A \|_p = \left(\sum_{k=1}^s \sum_{i=1}^m \sum_{j=1}^n | a_{ij}^{(k)} |^p \right)^{\frac{1}{p}}, \text{ for } 1 < p < \infty.$$

Lemma 2.1.2. Let A be a matrix in m -by- n -by- s dimensional space then $\| A \|_p$ is a norm.

Proof. • $\|A\|_p \geq 0$ and $\|A\|_p = 0$ if and only if $A = 0$ (by the definition)

$$\bullet \quad \|\alpha A\|_p = \left(\sum_{k=1}^s \sum_{i=1}^m \sum_{j=1}^n |\alpha a_{ij}^{(k)}|^p \right)^{\frac{1}{p}} = (|\alpha|^p \sum_{k=1}^s \sum_{i=1}^m \sum_{j=1}^n |a_{ij}^{(k)}|^p)^{\frac{1}{p}} = |\alpha| \|A\|_p$$

• We have to show $\|A+B\|_p \leq \|A\|_p + \|B\|_p$ where $A, B \in \mathbb{C}^{m \times n \times s}$.

$$\begin{aligned} \|A+B\|_p^p &= \sum_{k=1}^s \sum_{i=1}^m \sum_{j=1}^n |a_{ij}^{(k)} + b_{ij}^{(k)}|^p; \text{ by the Minkowski inequality} \\ &\leq \sum_{k=1}^s \sum_{i=1}^m \left(\left(\sum_{j=1}^n |a_{ij}^{(k)}|^p \right)^{\frac{1}{p}} + \left(\sum_{j=1}^n |b_{ij}^{(k)}|^p \right)^{\frac{1}{p}} \right)^p \\ &\leq \sum_{k=1}^s \left(\left(\sum_{i=1}^m \sum_{j=1}^n |a_{ij}^{(k)}|^p \right)^{\frac{1}{p}} + \left(\sum_{i=1}^m \sum_{j=1}^n |b_{ij}^{(k)}|^p \right)^{\frac{1}{p}} \right)^p \\ &\leq \left(\left(\sum_{k=1}^s \sum_{i=1}^m \sum_{j=1}^n |a_{ij}^{(k)}|^p \right)^{\frac{1}{p}} + \left(\sum_{k=1}^s \sum_{i=1}^m \sum_{j=1}^n |b_{ij}^{(k)}|^p \right)^{\frac{1}{p}} \right)^p \\ &= (\|A\|_p + \|B\|_p)^p \end{aligned}$$

□

The special case ($p = 2$) of p -norm is the Frobenius norm of $A \in \mathbb{C}^{m \times n \times s}$, and it can be defined as follow.

Definition 2.1.4. The Frobenius norm of $A \in \mathbb{C}^{m \times n \times s}$ is defined as follow:

$$\|A\|_F = \sqrt{\sum_{k=1}^s \sum_{i=1}^m \sum_{j=1}^n |a_{ij}^{(k)}|^2}.$$

Definition 2.1.5. Let $A \in \mathbb{C}^{m \times n \times s}$ then 2-norm of A is defined as follow:

$$\begin{aligned} \|A\|_2 &= \max_{k=1, \dots, s} \left(\max_{\|x\|_2=1} \|A^{(k)}x\|_2 \right) = \sqrt{\lambda_{max}^k} \text{ where } \lambda_{max}^k \text{ is the largest} \\ &\text{eigenvalue of } (A^{(k)})^* A^k \text{ for all } k. \text{ Also, it can be defined as } \|A\|_2^2 = \max_k (\lambda_{max}^k) \text{ where} \\ &\lambda_{max}^k = \max (|(A^{(k)})^* A^k - \lambda_k I| = 0); (k=1, \dots, s). \end{aligned}$$

Lemma 2.1.3. The $\|A\|_2$ is a norm where $A \in \mathbb{C}^{m \times n \times s}$.

Proof. • $\|A\|_2 = \sqrt{\max(\lambda_{max}^k)} \geq 0$ (since all eigenvalues of $(A^{(k)})^* A^k$ are real and non-negative) and $\|A\|_2^2 = 0 \Rightarrow A = 0$

- $\| \alpha A \|_2^2 = \max_k (\widetilde{\lambda}_{max}^k) = \max_k \{ \max (((\alpha A)^{(k)})^* \alpha A^k - \widetilde{\lambda}_k I) \}$ where $\widetilde{\lambda}_k$ is the eigenvalue of $(\alpha A^{(k)})^* \alpha A^k$.

Also we know from the definition $\| A \|_2 = \max_k \{ \max ((A^{(k)})^* A^k - \lambda_k I) \}$ where λ_k is the eigenvalue of $(A^{(k)})^* A^k$.

$$\begin{aligned}
(\alpha A^{(k)})^* \alpha A^k x &= \widetilde{\lambda}_k x \\
(A^{(k)})^* \alpha^* \alpha A^k x &= \widetilde{\lambda}_k x \\
(A^{(k)})^* \alpha^2 A^k x &= \widetilde{\lambda}_k x \\
\alpha^2 (A^{(k)})^* A^k x &= \widetilde{\lambda}_k x \\
\alpha^2 \lambda_k x &= \widetilde{\lambda}_k x \\
(\alpha^2 \lambda_k - \widetilde{\lambda}_k) x &= 0; \quad (x \neq 0 \text{ vector}) \\
\widetilde{\lambda}_k &= \alpha^2 \lambda_k
\end{aligned}$$

Finally; $\| \alpha A \|_2^2 = \max_k (\widetilde{\lambda}_{max}^k) = \max_k (\alpha^2 \lambda_{max}^k) = \alpha^2 \max_k (\lambda_{max}^k) = \alpha^2 \| A \|_2^2$
 $\Rightarrow \| \alpha A \|_2 = | \alpha | \| A \|_2$

- We have to show $\| A + B \|_2 \leq \| A \|_2 + \| B \|_2$ where $A, B \in \mathbb{C}^{m \times n \times s}$ and $A^k, B^k \in \mathbb{C}^{m \times n}$.

$$\begin{aligned}
\| A + B \|_2 &= \max_{k=1, \dots, s} \left(\max_{\|x\|_2=1} \| (A^{(k)} + B^{(k)})x \|_2 \right) \\
&= \max_{k=1, \dots, p} \left(\max_{\|x\|_2=1} \| A^{(k)}x + B^{(k)}x \|_2 \right) \\
&\leq \max_{k=1, \dots, s} \left(\max_{\|x\|_2=1} (\| A^{(k)}x \|_2 + \| B^{(k)}x \|_2) \right) \\
&\leq \max_{k=1, \dots, s} \left(\max_{\|x\|_2=1} \| A^{(k)}x \|_2 \right) + \max_{k=1, \dots, s} \left(\max_{\|x\|_2=1} \| B^{(k)}x \|_2 \right) \\
&= \| A \|_2 + \| B \|_2
\end{aligned}$$

□

2.2 Impression Matrix Norm

Solutions for dynamic large data sets are important in financial markets. Investors would like to tune their positions according to the real time market impression under fluctuating market price, volatility and interest rate. It is hard to deal with lots of variables at the same time. Therefore, it is necessary to define a proxy to reflect the

market impression quickly. We consider a 3-dimensional matrix having time, interest rate (r), and stochastic volatility dimensions where matrix entries are market prices. As an application of 3-dimensional norms we define impression matrix norm [6].

Table 2.1 : Simulation parameters.

$t = 0$; the initial time	$T = 1$; the terminal time -in years	$N = 1000$; number of paths
$q = 0$; the dividend yield	$\Delta t = 0.01$; the uniform mesh size	$\rho = 0.7$; the correlation coefficient
$n = 100$; the number of discretization points between 0 and T	$K = 4$; the rate of mean reversion	$\xi = 0.001$; the volatility parameters of variance process
$S_0 = 51.340,96$; the initial stock price		

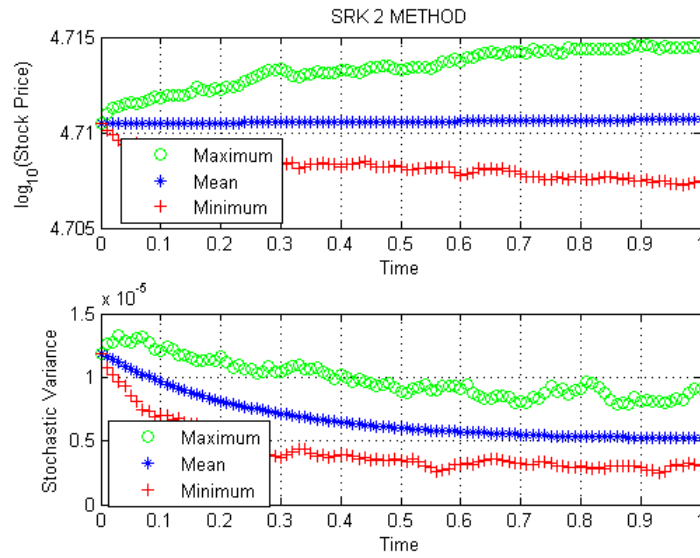


Figure 2.1 : One thousand realizations of simulation when $r = 7.5\%$, $v_0 = 119 \times 10^{-7}$ and $\theta = 52 \times 10^{-7}$.

Definition 2.2.1. Let $A \in \mathbb{C}^{m \times n}$ be a matrix. The 2-D row-wise moving matrix $M \subset A$ is defined as follows:

$$M = A[i : i + a - 1, :], i = 1, 2, 3, \dots, m - a + 1, M \in \mathbb{C}^{a \times n}$$

where a represents the number of row-wise sub-interval. The colon ":" refers to all the elements in the column of a matrix. Similarly, the column-wise moving matrix $B \subset A$ is defined as:

$$B = A[:, j : j + a - 1], j = 1, 2, 3, \dots, n - a + 1, B \in \mathbb{C}^{m \times a}$$

where a represents the number of column-wise sub-interval. The colon ":" refers to all the elements in the row of a matrix.

Definition 2.2.2. If $A \in \mathbb{C}^{m \times n \times s}$ then the 3-D row-wise moving matrix $C \subset A$ is defined as follows:

$$C = A[i : i + a - 1, :, :], i = 1, 2, 3, \dots, m - a + 1, C \in \mathbb{C}^{a \times n \times s}$$

where a represents the number of row-wise sub-interval. While the first colon ":" refers to all the elements in the second dimension, the second colon ":" refers to all the elements in the third dimension of the matrix A .

Analogously, 3-D moving matrices in other dimensions can be defined as well. Now, we define impression matrix norm (IMN) as a norm of the moving matrix with respect to time. IMN is generated by evaluating the norm of the matrix at each related time sub-interval. IMN of the 3-D matrix gives us a good picture of all the 3-D matrix data, and helps us to understand and interpret 3-D matrix more easily.

We believe that the impression matrix norms are useful for various time dependent data sets. When we consider financial applications using Heston model, we need to choose parameters so that they can satisfy the Feller condition $2\kappa\theta \geq \xi^2$ where non-negativity of volatility can be guaranteed [14] and we may deal with financially meaningful model realizations.

For example, we examine BIST-100 data between 02.01.2012 – 31.12.2012 and used the parameters in table 2.1, accordingly. We perform the simulations with the daily initial (v_0) and long term (θ) variances and obtain the graph in figure 2.1 by using the parameters in table 2.1. In the top panel of figure 2.1 fluctuation of stock price is presented. It shows that the model may not promise much valuable information for a long time scale since the effect of the initial information is decreased as time passes. In the bottom panel of figure 2.1 the mean reversion property for the variance process is presented. It starts from initial variance level and reverts to the long term variance level as it is expected from the Heston model.

2.3 Simulations Results

2.3.1 Scenarios: Randomly generated interest rates

Interest rates generally change randomly at the real market. Therefore, we have to take this situation account in order to converge the real market behavior by this

aspect. For this purpose, we focus on two different interest rates scenarios when we perform extensive simulations. We obtain these scenarios as follows. We start with initial interest rate as %8, which presents in table 2.2, and generate 280 new random interest rates by adding random number within $\%[-2, 2]$ and $\%[-10, 10]$ to the previous interest rate at each step for the first and second scenarios, respectively. Here, we present some graphics obtained from simulations by using the parameters in table 2.2 and the interest rates for the second scenario via Euler-Maruyama, Milstein and Stochastic Runge-Kutta methods. Firstly, we obtain graphs in figure 2.2 which show price evolution in 3-D at the left panel and the fluctuations of variance and stock price by the time at the right panel.

Table 2.2 : Parameters for different interest rates scenarios.

$t = 0$; the initial time	$T = 1$; the terminal time -in years	$N = 1000$; number of paths	$n = 100$; the number of discretization points between 0 and T
$q = 0$; the dividend yield	$\Delta t = 0.01$; the uniform mesh size	$S_0 = 10$; the initial stock price	$r_0 = 0.08$; the interest rate
$\rho = 0.7$; the correlation coefficient	$K = 4$; the rate of mean reversion	$\theta = 0.3$; the long run variance	$\xi = 0.1$; the volatility parameters of variance process
$v_0 = 0.4$; the initial variance			

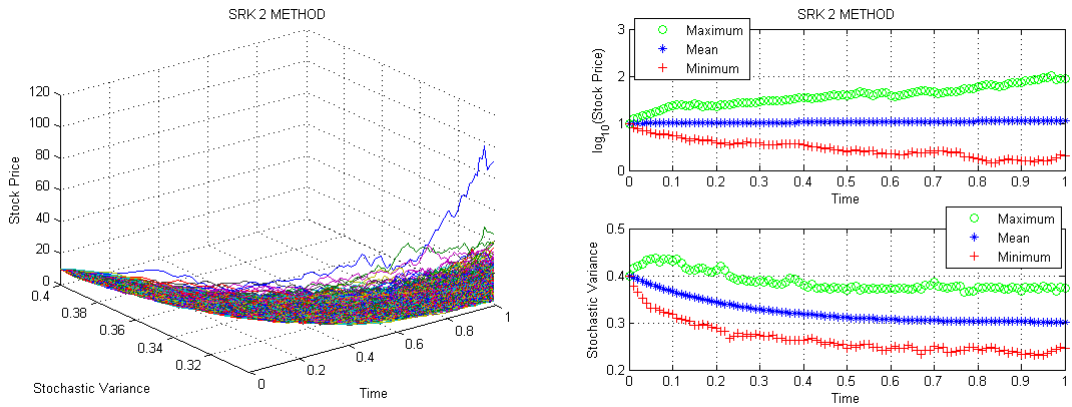


Figure 2.2 : One thousand realizations of simulation for second scenario.

After that, we get 3-dimensional stock price expectation matrix M ($M \in \mathbb{C}^{1000 \times 101 \times 280}$). If we use IMN in the 2-norm to analyze M , as an example we select the length of time sub-intervals as 0.01 year and the number of time sub-interval as 3, then we obtain the graphs in figure 2.3, figure 2.4 and figure 2.5. We observe that the norm values at the terminal time can be ordered by the inverse relation with the rates of convergence of the methods.

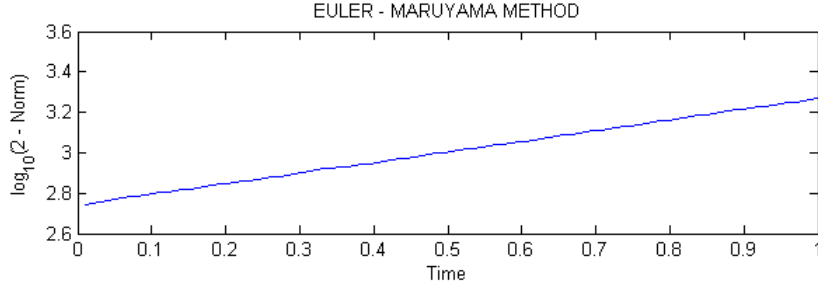


Figure 2.3 : Impression norm of matrix M for second scenario by Euler - Maruyama method.

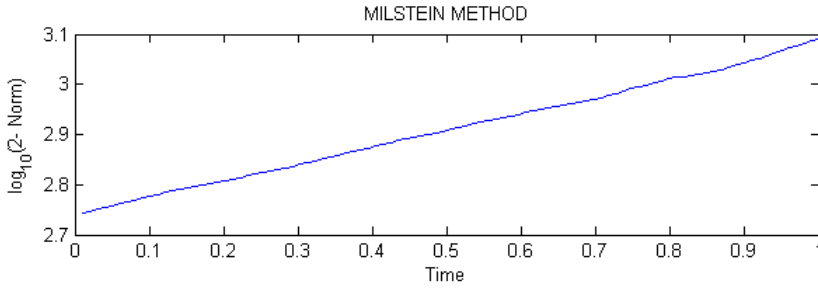


Figure 2.4 : Impression norm of matrix M for second scenario by Milstein method.

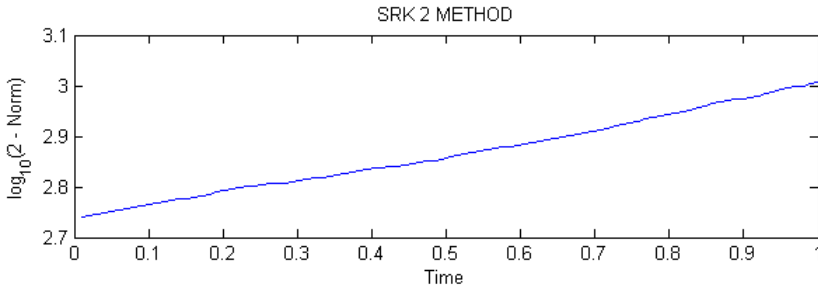


Figure 2.5 : Impression norm of matrix M for second scenario by stochastic Runge-Kutta method.

We can summarize the analyses results for the both scenarios with the table 2.3. These results show that there is an inverse relationship between rates of convergence of the numerical methods and the norm values which are obtained for each of the method.

2.3.2 Volatility in terms of extreme values

Overlapping Case: Let S_t denote the stock price at time t. Duran [29] defines the volatility of stock price on Day i , with a memory of the most recent $\phi + 1$, for example 25, trading days, by

$$v_{S_i} = \left(\max_{i-\phi \leq t \leq i} S_t - \min_{i-\phi \leq t \leq i} S_t \right) / \min_{i-\phi \leq t \leq i} S_t. \quad (2.1)$$

Table 2.3 : Average values of norms obtained by using randomly generated interest rates.

According to new interest rates which are updated within % [-2, 2] randomly at each step			
Mean ($\log_{10}(\text{IMN})$)	Euler	Milstein	SRK
1-norm	3.9874	3.9863	3.9221
2-norm	2.8494	2.8489	2.7785
Inf-norm	6.4681	6.4641	6.4022
Fro-norm	4.0357	4.0322	3.9686

According to new interest rates which are updated within % [-10,10] randomly at each step			
Mean ($\log_{10}(\text{IMN})$)	Euler	Milstein	SRK
1-norm	4.0396	4.0165	3.9647
2-norm	2.9506	2.9095	2.8626
Inf-norm	6.5227	6.4928	6.4486
Fro-norm	4.0901	4.0612	4.0171

Unit volatility at the overlapping case: Let S_t denote the stock price at time t . The unit volatility of stock price is defined on Day i as

$$v_{S_i} = \frac{\max_{i-\phi \leq t \leq i} S_t - \min_{i-\phi \leq t \leq i} S_t}{(\phi + 1) \left(\min_{i-\phi \leq t \leq i} S_t \right)}. \quad (2.2)$$

on a time interval whose length is $\phi + 1$ (with a memory of the most recent $\phi + 1$), for example 25, trading days.

When we apply (2.1) and (2.2) to the BIST-100 data set, we obtain volatility (σ) and approximate variance ($\approx \sigma^2$) of BIST-100 for each year as shown in the table 2.4.

Table 2.4 : Volatilities in terms of extreme values.

Time interval	Number of trading days	Max BIST-100	Min BIST-100	Volatility	Variance	Dailiy volatility	Daily variance
04.01.2007-31.12.2007	252	58.231,90	36.629,89	0,59	0,35	0,0023402	0,0000055
02.01.2008-31.12.2008	251	54.708,42	21.228,27	1,58	2,49	0,0062835	0,0000395
02.01.2009-31.12.2009	252	52.825,02	23.035,95	1,29	1,67	0,0051316	0,0000263
04.01.2010-31.12.2010	250	71.543,26	48.739,43	0,47	0,22	0,0018715	0,0000035
03.01.2011-30.12.2011	253	70.072,02	49.621,67	0,41	0,17	0,0016290	0,0000027
02.01.2012-31.12.2012	253	78.579,08	49.836,98	0,58	0,33	0,0022795	0,0000052

2.3.3 Real data applications

For the real data application of the Heston model, we use 253 daily interest returns between 02.01.2012 – 31.12.2012 (see figure 2.6) and the initial stock price as 51.340,96 TRY from BIST-100 on 02.01.2012 (see figure 2.10). We obtain an

approximate initial volatility level (on 02.01.2012) as an average of the last 5 years' volatilities by using the data in table 2.4.

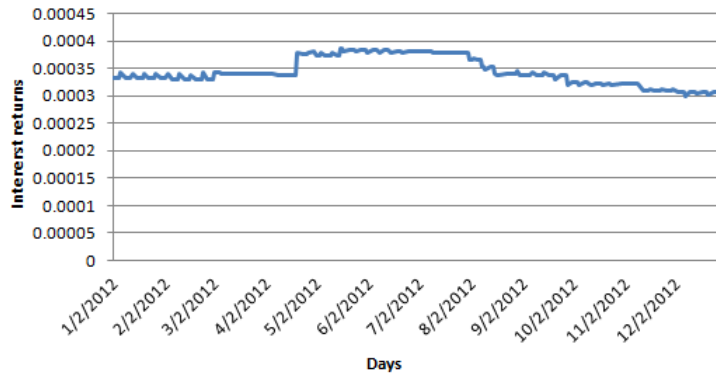


Figure 2.6 : Daily interest returns between 02.01.2012 and 31.12.2012.

At this step we perform analyses for two different initial volatilities with the corresponding long run volatilities. The first analysis is done for the annual volatility whose initial volatility level on 02.01.2012 obtained from the average of the annual volatilities between 2007 and 2011 in the 5th column of the table 2.4. The average of the daily volatilities between 2007 and 2011 in the 7th column of the table 2.4 is used to approximate the initial daily volatility level on 02.01.2012 for the second analysis. We use approximate long run volatility levels as 0.58 for the annual volatility and 228×10^{-5} for the daily volatility as in table II for 2012. The corresponding approximate long run variance levels between 02.01.2012 and 31.12.2012 are evaluated by taking square of these volatility values (i.e. long run annual variance is approximately $(0.58)^2 \approx 0.33$ & long run daily variance is approximately $(228 \times 10^{-5})^2 \approx 52 \times 10^{-7}$).

Then, we perform simulations for these values by using the parameters in table 2.1 and obtain 3-dimensional stock price expectation matrix M ($M \in \mathbb{C}^{1000 \times 101 \times 253}$). Now, for example, let us select the length of time sub-intervals as 0.01 year (i.e. approximately 2.53 trading days) and the number of time sub-interval as 3. Afterwards, we use IMN in the 2-norms for M to analyze and quantify price impression approximately and obtain the graphs in figure 2.7, figure 2.8 and figure 2.9. These graphs show almost parallel behaviors to the graph of BIST-100 index between 02.01.2012 – 31.12.2012 which is shown in figure 2.10.

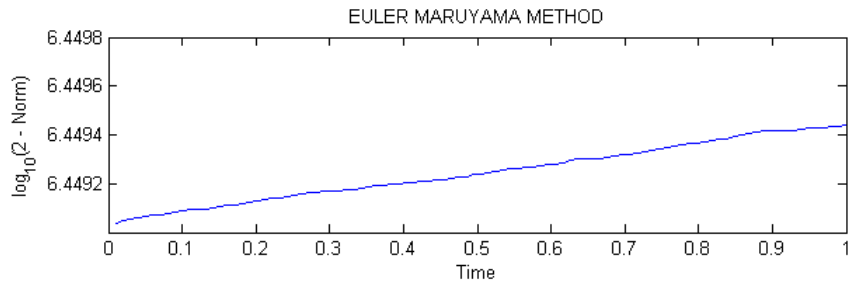


Figure 2.7 : Impression norm of matrix M for daily volatility by Euler - Maruyama method.

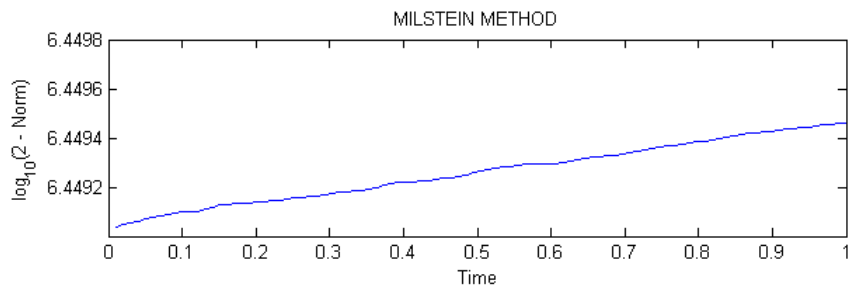


Figure 2.8 : Impression norm of matrix M for daily volatility by Milstein method.

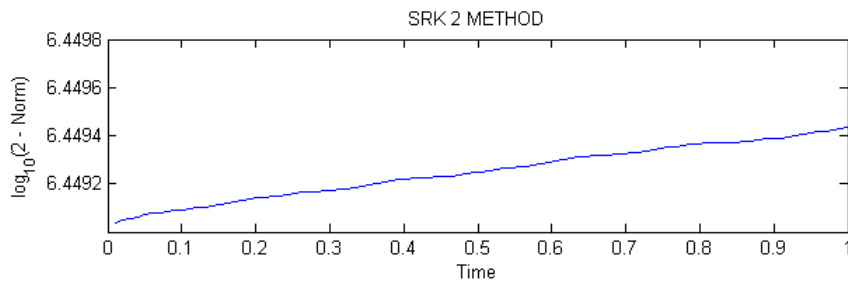


Figure 2.9 : Impression norm of matrix M for daily volatility by stochastic Runge-Kutta method.



Figure 2.10 : BIST-100 between 02.01.2012 and 31.12.2012.

When we estimate the numerical solutions of stochastic differential equations, simulation methods and their rates of convergence are important. Practitioners generally choose methods which is faster than the others especially when concerned with financial markets since investment timing is important. For this purpose, we perform simulations with Euler Maruyama, Milstein and stochastic Runge-Kutta methods to compare their advantages and limitations using the 3-dimensional norms. These methods are consistent and stable [15, 16, 19].

Application of the Euler Maruyama (with 0.5 strong order) and Milstein (with 1 strong order) methods are almost similar and they are generally used by the practitioner since their applications to the stochastic differential equations are easy.

Burrage and Burrage [17] consider the high strong order explicit stochastic Runge Kutta Methods (see [17] and references therein). We use explicit SRK method with strong order 2 in our analysis. On the other hand, Mitsui, Burrage and Burrage showed implementation and stability issues of the numerical solutions of stochastic differential equations in their paper. Stochastic Runge-Kutta methods for solving stochastic differential equations are efficient and consistent. They also have good precision and stability (see [18–20] and references therein).

Table 2.5 : Average values of norms obtained by using the annual volatility at the overlapping case.

Mean(IMN)	Euler	Milstein	SRK
1-norm	4,3121E+07	4,2778E+07	3,6732E+07
2-norm	3,3966E+07	3,3808E+06	2,8541E+06
Inf-norm	1,2992E+10	1,2984E+10	1,1129E+10
Fro-norm	5,0576E+07	5,0525E+07	4,3077E+07

Table 2.6 : Average values of norms obtained by using the daily volatility at the overlapping case.

Mean(IMN)	Euler	Milstein	SRK
1-norm	3,8996E+07	3,8996E+07	3,8996E+07
2-norm	2,8135E+06	2,8135E+06	2,8135E+06
Inf-norm	1,2994E+10	1,2994E+10	1,2994E+10
Fro-norm	4,4744E+07	4,4744E+07	4,4744E+07

We observe from the table 2.5 that there is an inverse relationship between rates of convergence of the numerical methods and the norm values which are obtained for each of the method when we use the initial and long term annual volatilities. The

results can be explained by the cumulative error of the numerical methods. In other words, the cumulative error decreases as the order of convergence increases, consistent with the literature [15, 16, 19]. On the other hand, in the daily volatilities case, the results in table 2.6 show that the model reflects the effect of the low volatilities, when the initial and long term daily volatilities are very small for the BIST-100 large data set. Consequently, we can interpret the results in table 2.6 as the rate of convergence of the methods can not be more dominant than small volatility situations while performing the simulations. Given similar robustness one may prefer Euler Maruyama method because of its lowest cost compared to Milstein and SRK methods [6].

3. EXTREME VALUE ANALYSIS AND ITS APPLICATION IN FINANCE

3.1 Application of Extreme Value Theory on Heston Model

It is hard to find one single model to capture all kinds of behaviors in stock markets. Therefore, it is valuable to examine strengths and weaknesses of related mathematical models or approaches. In this chapter, we focus on 3D extreme value analysis for the average logarithmic stock return, interest rate and speed of mean reversion variables from the Heston stochastic volatility model [3] which may capture limited kinds of behaviors and may reflect fat-tails and high peaks in the logarithmic return distributions under different market situations. We conduct various simulations using numerical solutions of the stochastic differential equations (SDEs) with different parameters via Milstein method [16, 19]. We provide an extensive tail behavior analysis of the daily logarithmic stock return distributions for some of the model parameters with respect to the extreme value based analysis. We also analyze the daily logarithmic return distributions of the Borsa Istanbul - 100 (BIST-100) index between 02.01.2004 and 17.06.2013. On the other hand, Duran and İzgi discuss the extreme situations using extreme value theory in [7] by 3D perspective. Moreover, it is important to analyze and distinguish the comovement and polarization of the time dependent variables in financial markets. We are interested in the comovement and polarization of interest rates and daily returns of BIST-100 index between 2010 and 2013 [7, 31].

Initial variance, long term variance and speed of mean reversion are some of the main characteristic parameters of the Heston stochastic volatility model. We use Parkinson extreme value method while we estimate variances of BIST-100 index for each year between 02.01.2004 and 31.12.2012. After that, we perform simulations and generate quantile-quantile plot (QQ-plot), mean excess function against the the different thresholds plot (ME-plot) and Hill-plot of the logarithmic stock return distributions as an application of the extreme value theory. Then, we present and quantify fat-tailness of the logarithmic stock return distributions by using QQ-plot,

ME-plot and Hill-plot. Furthermore, we make some of the parameters analysis of Heston model. In particular, we examine 3D dynamics of the average logarithmic stock return, interest rate and speed of mean reversion variables for the various market situations such as flight to more stable or more unstable situations. Heston stochastic volatility model suggests that the average logarithmic stock return increases as interest rate increases. On the other hand, it is important to find polarization domains where comovement of financial variables may turn out to be distant from each other (see Bommarito and Duran [32] and references therein). Therefore, we check that whether there are also sufficiently large time intervals where the Heston stochastic volatility model may not work in terms of interest rates and daily returns in real data.

3.1.1 Extreme value theory

Extreme value theory has a importance role to explain and predict probability of extreme events in many disciplines. Finance, economics, earth science, climatology and hydrology are some of the applicability area for the extreme value theory. Embrechts et al. [33] have very important study of extreme value theory to finance and insurance literature. Reiss and Thomas [34], Beirlant et. al. [35] have extensive works on statistical analysis of extreme values. Huisman et. al. [36] and Mcneil [37] are also have important works about extreme value theory and tail estimates, among others.

In finance literature, it is expected that the stock price has log-normal distribution. On the other hand, the financial returns (i.e. stock returns) are expected to have normal distribution which may have fat-tail or heavy-tail. We use main characteristics of the distributions such as mean, variance, standard deviation, skewness and kurtosis etc. at the statistical analyses. Especially, the kurtosis (or the fourth standardized moment) can be used to catch some clue about the tail behavior of the distributions although it is not enough to explain fat-tailness of the distribution [33, 38]. At this point, extreme value theory based analyses help us to study the tail behavior of the distributions.

First of all, we need to give the definition of the fat-tailness (or heavily tailness) of a distribution whose definition is not unique in the literature [33]. We assume distributions have fat-tail if their density functions have power decay at the tail region otherwise they have thin-tailness (i.e. exponential decay or a finite end points, [38]).

In the extreme value theory and its applications; histogram of the distribution, the quantile-quantile plot (QQ-plot) and mean excesses against the thresholds plot are frequently used tools to examine the fat-tailness of the distributions [34]. QQ-plot is useful tool to compare quantiles of the empirical distribution with the hypothesized distribution. The quantiles of the empirical distribution are generally plotted against the exponential distribution to quantify fat-tailness of the distribution at the extreme value theory analysis. If the empirical data comes from reference distributions, then QQ-plot is expected to be almost linear. At the tail region, concave departure from straight line is an indication of the fat-tailed distribution while convex departure is an indication of thin tailed distribution when the hypothesized's and empirical distributions quantiles are on the vertical and horizontal axis, respectively [33].

On the other hand, mean excess plot (ME-plot) is the representation of the mean excess function. The mean excess function of the random variable X is defined as follow:

$$e(u) = E[X - u | X > u], 0 \leq u < X_F$$

where u is the sufficiently high threshold and X_F is the right endpoint. Shortly, the mean excess function evaluate the average of the excesses over the threshold and it can be used as an indicator of fat-tailness of the distribution if it has positive slope (for more details please see [33, 34]).

The other important tool is Hill-plot which is used to evaluate shape parameter $\xi = \frac{1}{\alpha}$ where α is the tail index. The shape parameters $\xi = 0$ (Gumbel distribution), $\xi > 0$ (Fréchet distribution) or $\xi < 0$ (Weibull distribution) indicate an exponentially decaying, power-decaying, or finite-tail distributions in the limit, respectively. By the Hill-plot aspect, empirical distributions may have fat-tail when $\xi > 0$, according to the definition of the fat-tailed distribution. The shape parameter ξ needs to be choosen at the relatively stable area at the Hill-plot [33, 37, 39]. Consequently, we use histogram of the distributions with the best fitted normal distribution, QQ-plot, ME-plot and Hill-plot when we examine fat-tailness of the empirical distributions by using the EVIM software [40].

3.1.2 High peak and fat tail analysis for the model parameters

We investigate some of the model parameters effect for the high peak and fat-tail analysis while we perform simulations with Heston stochastic volatility model for

BIST-100 between 02.01.2012 and 31.12.2012. We focus on behavior of the logarithmic stock returns (i.e. $r_i = \log(S_i/S_{i-1})$ where the S_i represents the stock price) at our analysis. When we consider financial applications using Heston model, we need to choose parameters so that they can satisfy the Feller condition $2\kappa\theta \geq \xi^2$ where non-negativity of volatility can be guaranteed [14] and we may deal with financially meaningful model realizations. For example, we examine BIST-100 data between 02.01.2012 – 31.12.2012 and used the following parameters while we conduct simulations: $t = 0$ (the initial time), $T = 1$ (terminal time), $n = 100$ (the number of discretization point between 0 and T), $\Delta t = 0.01$ (the uniform mesh size), $N = 1000$ (the number of paths), $q = 0$ (dividend yield), $\xi = 0.01$ (volatility parameters of variance process) and $S_0 = 51.340,96$ (the initial stock price).

Moreover, we use the Parkinson extreme value method [28] when we estimate variances of the BIST-100 index for each year between 01.02.2004 and 31.12.2012. The Parkinson's method suggested that using the natural log of the ratio of highest to lowest price in the interval as a better estimator of volatility than the traditional volatility measure and the standard deviation. We also evaluate the approximate daily volatility by dividing the annual volatility value to the length of time interval where it is estimated with the Parkinson method. As a result, we obtain daily volatilities (σ) with the corresponding approximate variances ($\approx \sigma^2$) of BIST-100 for each year as shown in the table 3.1.

Table 3.1 : Daily volatilities and variances in terms of extreme values.

Time interval	Number of trading days	Max BIST-100	Min BIST-100	Daily volatility	Daily variance
02.01.2004-29.12.2004	249	24.971,68	15.922,44	0,0365881	0,0013387
03.01.2005-30.12.2005	254	39.837,27	23.285,94	0,0382450	0,0014627
02.01.2006-29.12.2006	250	47.728,50	31.950,56	0,0386655	0,0014950
04.01.2007-31.12.2007	252	58.231,90	36.629,89	0,0396053	0,0015686
02.01.2008-31.12.2008	251	54.708,42	21.228,27	0,0415088	0,0017230
02.01.2009-31.12.2009	252	52.825,02	23.035,95	0,0408805	0,0016712
04.01.2010-31.12.2010	250	71.543,26	48.739,43	0,0401387	0,0016111
03.01.2011-30.12.2011	253	70.072,02	49.621,67	0,0392322	0,0015392
02.01.2012-31.12.2012	253	78.579,08	49.836,98	0,0405775	0,0016465

We believe that Heston model can reflect limited kinds of fat-tails and high peaks in the daily stock return distributions under various market situations. Before we perform the simulations of the Heston model we need initial daily variance level, as well. We obtain approximate initial daily volatility level (on 02.01.2012) as an average of the daily volatilities between 2004 and 2011 in the 5th column of the table 3.1. After that, we

evaluate the corresponding initial daily variance level as 155×10^{-5} by taking square of this volatility. Furthermore, we use long run daily variance level approximately 165×10^{-5} (i.e. square of the daily volatility) for 2012 as it is shown in table 3.1. Then, we start to make an analysis of fat-tailness and high peaks for the different correlation coefficients (ρ), between Brownian motions of asset price process and the variance process, such that $\rho = 0.8$ and $\rho = -0.8$ while the speed of mean reversions (κ) are 0.1, 1, 2, 3, 4, 5, 6 and the interest rate (r) is 7.5%. We present some of the figures of the distributions for the logarithmic stock return obtained from the simulations.

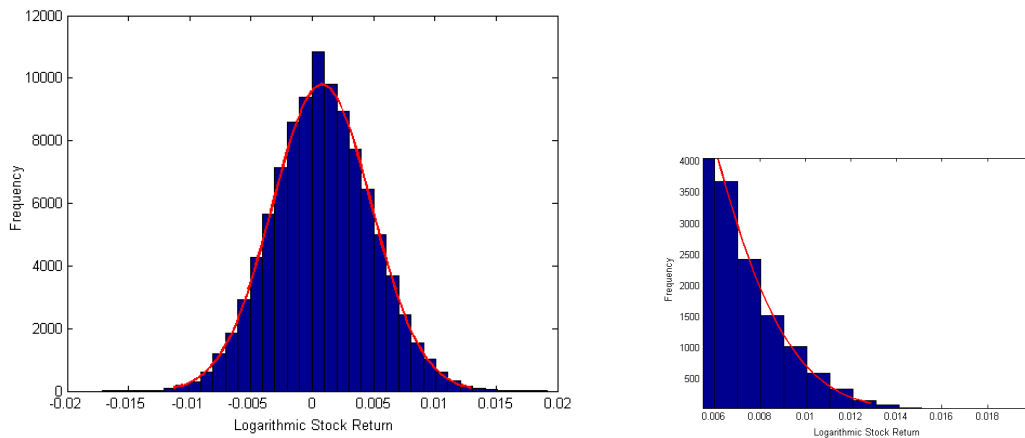


Figure 3.1 : Distribution of logarithmic stock return when $r = 7.5\%$, $\kappa = 6$ and $\rho = 0.8$.

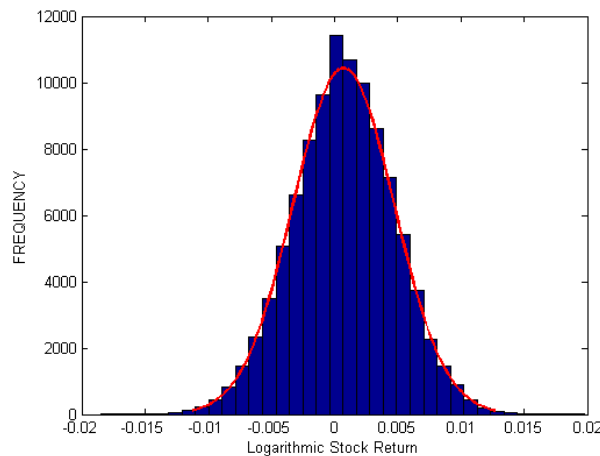


Figure 3.2 : Distribution of logarithmic stock return when $r = 7.5\%$, $\kappa = 0.1$ and $\rho = -0.8$.

At the left panel of the figure 3.1, the distribution of the logarithmic stock return with the best fitted normal distribution is presented while the right tail is zoomed at the right panel for the positive correlation coefficient. Similarly, the figure 3.2 represents the distribution for the logarithmic stock return for the negative correlation coefficient.

Table 3.2 : Statistics for distributions of logarithmic stock return for positive correlation coefficient.

K	0.1	1	2	3	4	5	6
Mean	0,002274	0,001878	0,001555	0,001321	0,001151	0,001051	0,000989
Maximum	0,01921	0,01884	0,01853	0,01831	0,01814	0,01806	0,01802
Minimum	-0,01466	-0,01509	-0,01543	-0,01566	-0,01583	-0,01595	-0,01604
Std. Dev.	0,01075	0,01077	0,01078	0,01078	0,01078	0,01079	0,01081
Range	0,03386	0,03393	0,03396	0,03397	0,03397	0,03401	0,03405
Kurtosis	3,1075	3,0753	3,0592	3,0511	3,0465	3,0435	3,0414
Skewness	0,0612	0,0611	0,0612	0,0614	0,0615	0,0616	0,0617

We obtain table 3.2 and table 3.3 for the quantitative information which help us to understand and explain behavior of the distributions more easily. We observe from the table 3.2 that the mean, maximum and minimum values of the logarithmic stock returns decrease while the rates of mean reversion increase for the positive correlation coefficient. We also observe from the table 3.3 that the mean and maximum values of logarithmic returns decrease and the minimum values almost increase for the negative correlation. Furthermore, these values for the positive correlation are larger than that of the negative correlation coefficient which is also in the line of the findings in Duran and İzgi [31].

Table 3.3 : Statistics for distributions of logarithmic stock return for negative correlation coefficient.

K	0.1	1	2	3	4	5	6
Mean	0,0006702	0,0003582	0,0002211	0,0002829	0,0001774	0,0000538	-0,0000460
Maximum	0,01859	0,01777	0,01726	0,01716	0,01706	0,01697	0,01689
Minimum	-0,01725	-0,01706	-0,01682	-0,01659	-0,01670	-0,01686	-0,01698
Std. Dev.	0,01137	0,01106	0,01082	0,01071	0,01072	0,01074	0,01075
Range	0,03584	0,03483	0,03408	0,03375	0,03376	0,03382	0,03387
Kurtosis	3,1165	3,0810	3,0624	3,0525	3,0466	3,0427	3,0401
Skewness	-0,0532	-0,0530	-0,0530	-0,0531	-0,0531	-0,0532	-0,0533

The standard deviations have almost same behaviors with the sign of the correlation coefficients. In other words, standard deviations almost increase for the positive correlation while they almost decrease for the negative correlation for the incremental values of κ . On the other hand, kurtoses are greater than 3 at the both cases. Although it can be interpreted as an indicator of the fat-tailness, as we mention at the extreme value theory section, it is not enough evidence for the fat-tailness of the distributions. It

represents that distributions of the logarithmic stock return have relatively high peaks for all values of κ and ρ while they have right and left skew for the positive and negative correlation coefficients, respectively.

Fat-tailness of the distributions is still uncertain case which needs to investigate more deeply by using the other methods. Extreme value theory's tools especially QQ-plot and mean excess function plot against to the different thresholds may explain the fat-tailness of the distributions. For this purpose, we generate the following graphs for some of the model parameters:

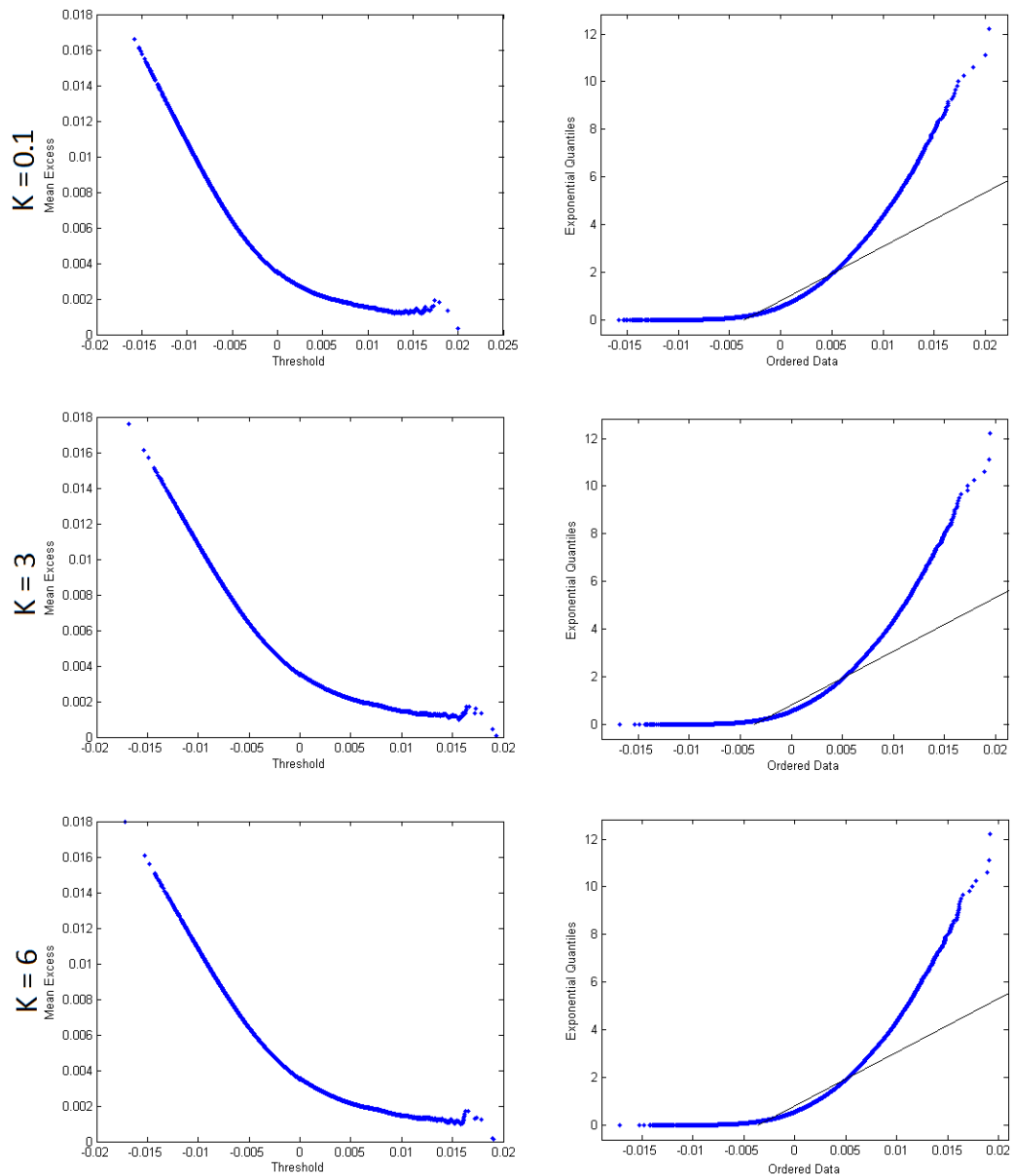


Figure 3.3 : Mean Excess (left) and QQ (right) plots for positive correlation coefficient.

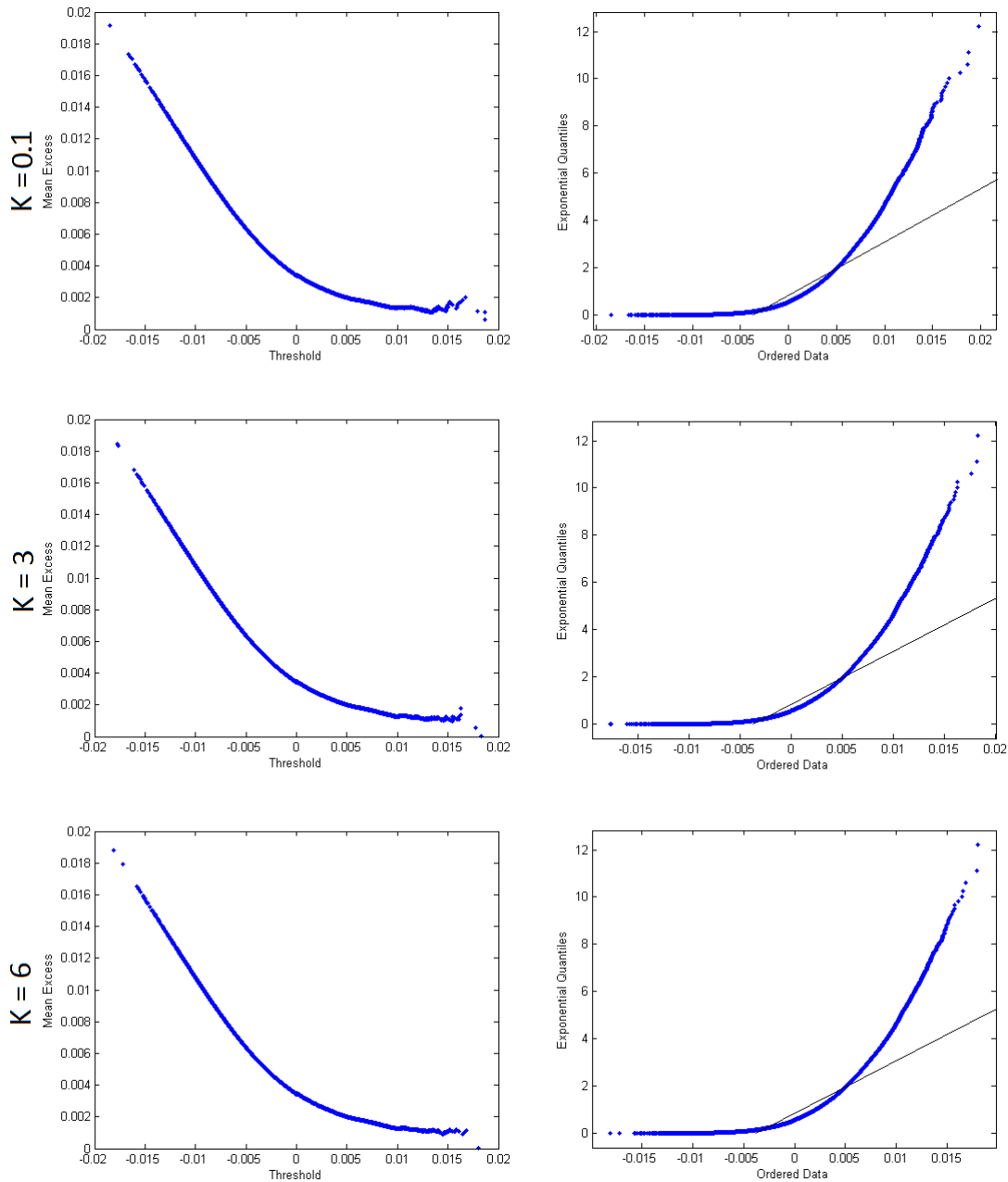


Figure 3.4 : Mean Excess (left) and QQ (right) plots for negative correlation coefficient.

The mean excess plots in the left panels of figure 3.3 and figure 3.4, which have positive uptrend for threshold values greater than approximately 0.015, indicate a heavy right tails for the logarithmic stock return distributions. We obtain from ME-plot that there is a positive relationship between its slope at the tail region and the speeds of mean reversion for the positive correlation. On the other hand, we observe that there is an inverse relationship between ME-plots slopes' at the tail region and the speeds of mean reversion for the negative correlation coefficient. Moreover, the QQ plots against the exponential distribution in the right panel of figure 3.3 and figure 3.4, where the

sufficiently large concave departure from linearity is presented at the right tail region, support evidences of fat-tailness of the underlying distributions.

For the shape parameters estimation we generate the Hill-plots of the empirical distributions for the various speed of mean reversion. The Hill-plots of the logarithmic stock return distributions with a 0.95 confidence interval are displayed in figure 3.5 and figure 3.6 for the positive and negative correlation coefficients, respectively. The relatively stable regions are indicated with the rectangular.

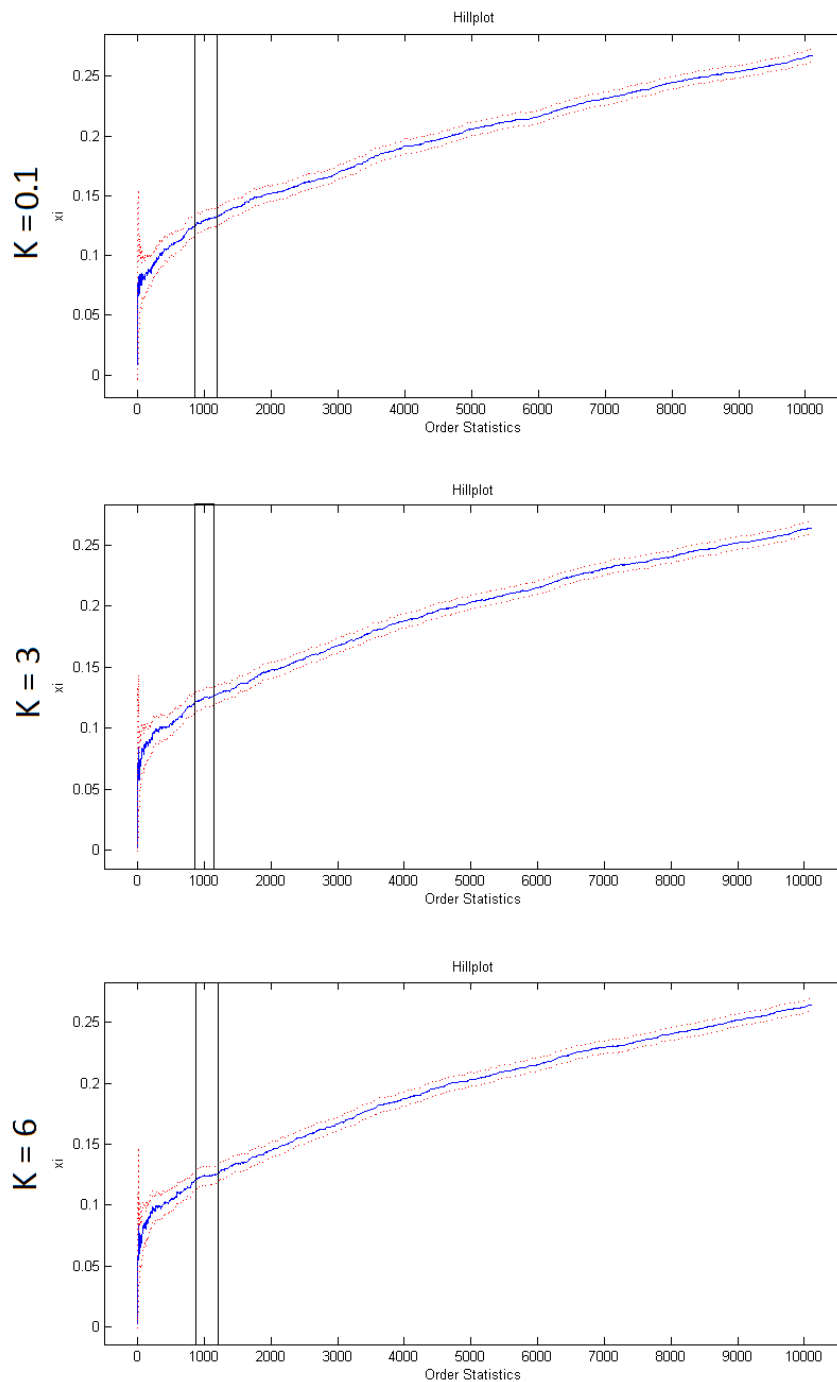


Figure 3.5 : Hill plots for positive correlation coefficients.

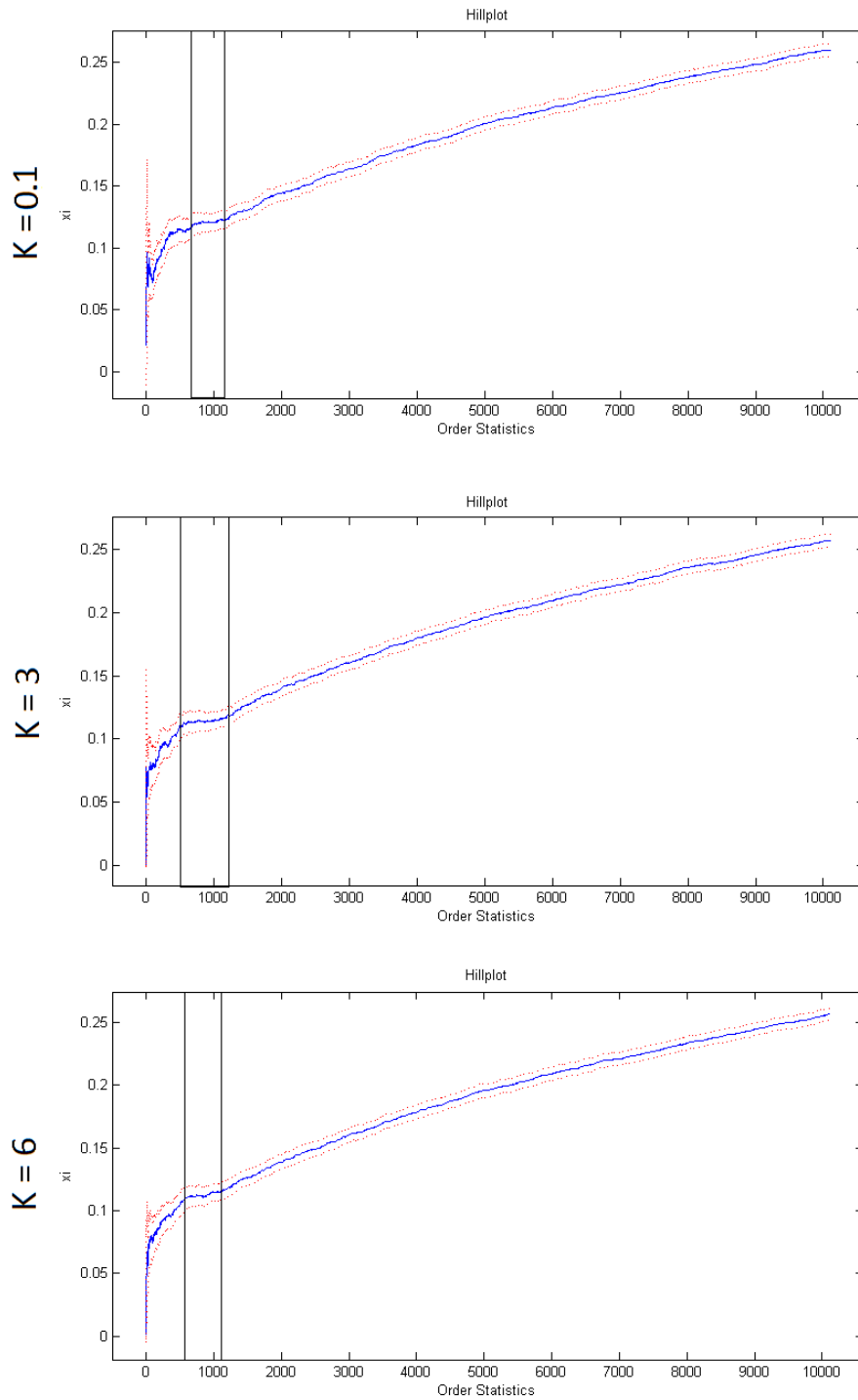


Figure 3.6 : Hill plots for negative correlation coefficients.

The shape parameters ξ estimate approximately between 0.12 and 0.13 for $\kappa = 0.1$ and between 0.11 and 0.12 for $\kappa = 3$ and 6 at the relatively stable regions in figure 3.5. Similarly, the shape parameters ξ estimate approximately between 0.119 and 0.121 for $\kappa = 0.1$, between 0.113 and 0.116 for $\kappa = 3$, and between 0.107 and 0.116 for $\kappa = 6$ at the relatively stable regions in figure 3.6. All the shape parameters are greater than zero ($\xi > 0$) which implies power-decaying tail and also heavy tail.

The power-decaying tail with an exponent tail index α varies between 7.7 and 8.3 for $\kappa = 0.1$, between 8.3 and 9.1 for $\kappa = 3$ and 6 for the positive correlation and similarly it varies between 8.3 and 8.4, between 8.6 and 8.9, between 8.6 and 9.3 for $\kappa = 0.1, 3, 6$, respectively, for the negative correlation coefficients. These tail index means that, for example $7.7 < \alpha < 8.3$, if the expectation of the logarithmic stock return greater than r is P then probability of the logarithmic stock return greater than $h \cdot r$ is in the $h^{-7.7}P$ and $h^{-8.3}P$.

Consequently, we present fat-tailness of the logarithmic stock return distributions, which are generated from the Heston stochastic volatility model via Milstein method, by using the QQ-plots, ME-plots and Hill-plots based on extreme value theory.

3.2 High Peak and Fat Tail Analysis for BIST-100

As a real data application, we analyze the fat-tailness and high-peaks of the daily logarithmic BIST-100 return distribution. We use large data set which include the daily closing of BIST-100 index between 02.01.2004 and 17.06.2013. There are 2380 observations in the data set. We start the analysis by obtaining some of the main characteristics of the data as shown in table 3.4.

Table 3.4 : Statistics for distribution of daily logarithmic BIST-100 returns, 2004 - 2013.

Mean	Maximum	Minimum	Std. Dev.	Range	Kurtosis	Skewness
0,005317	0,1192	-0,1086	0,06754	0,2278	6,238	-0,279

When we investigate loses of the BIST-100 (i.e. focus on the left tail of BIST-100 distribution, see figure 3.7) using extreme value theory, we need to analyze BIST-100 negative return distribution where the returns multiplied by -1 since the extreme value analysis works with the right tail of the distribution [40]. The histograms of the logarithmic BIST-100 returns and negative logarithmic BIST-100 returns with the best fitted normal distribution are displayed in the left panels of the figure 3.7 and figure 3.10 while the right tails are zoomed at the right panel of them. Although the logarithmic BIST-100 returns distribution has relatively low skewness -0.279 level (i.e. skewed to the left and the negative logarithmic BIST-100 returns has relatively low skewness 0.279 (i.e. skewed to the right) which can be obtained by using the fundamental properties of statistics), it also has relatively high kurtosis 6.238 value.

The kurtosis value may be interpreted as evidence of the high-peaks but it is not enough evidence for the fat-tailness. For this purpose, we get more extensive analysis with QQ-plot, ME-plot and Hill-plots.

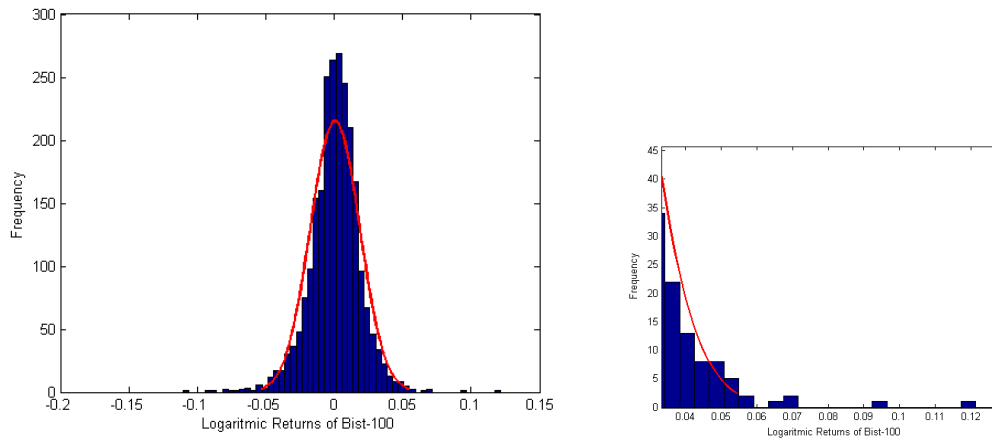


Figure 3.7 : Distributions of logarithmic BIST-100 returns between 02.01.2004 and 17.06.2013.

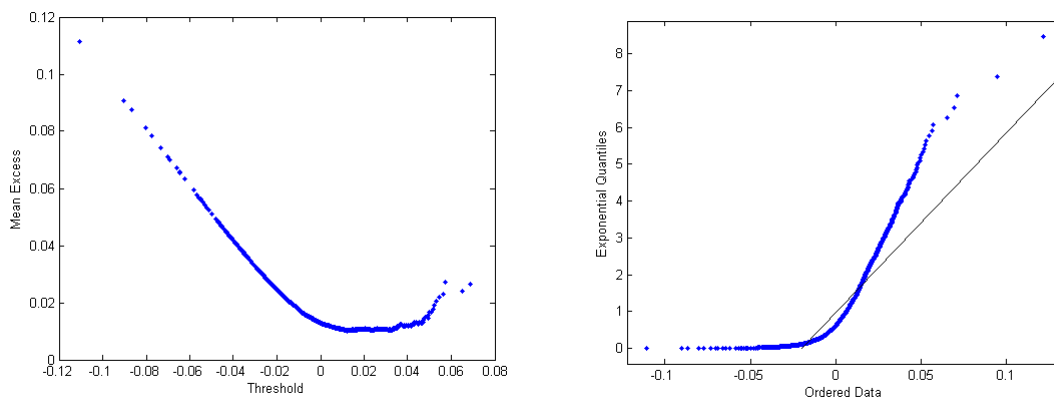


Figure 3.8 : ME (left) and QQ (right) plots of BIST-100 for the right tail, 2004 - 2013.

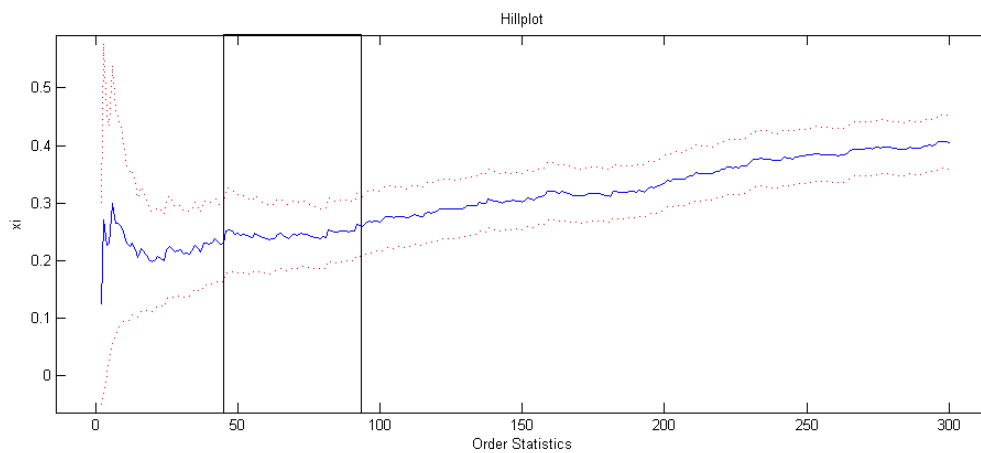


Figure 3.9 : Hill plot of BIST-100 for the right tail, 2004 - 2013.

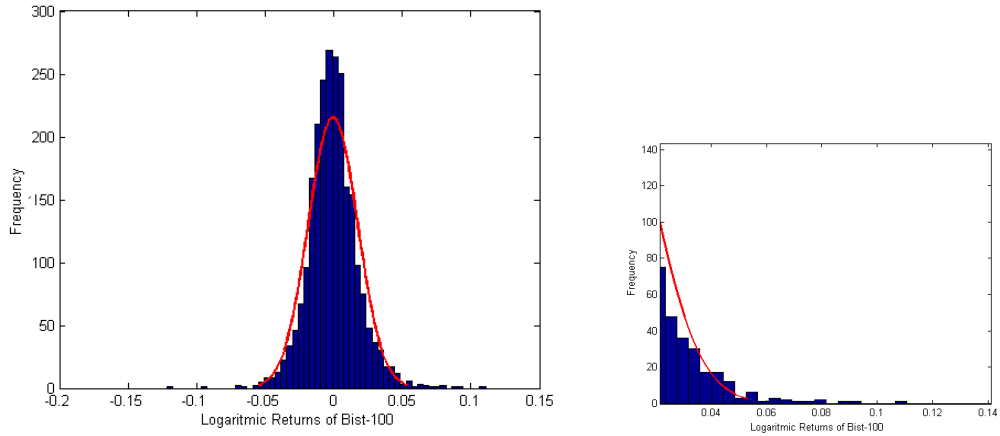


Figure 3.10 : Distributions of logarithmic BIST-100 (returns multiplied by -1) negative returns between 02.01.2004 and 17.06.2013.

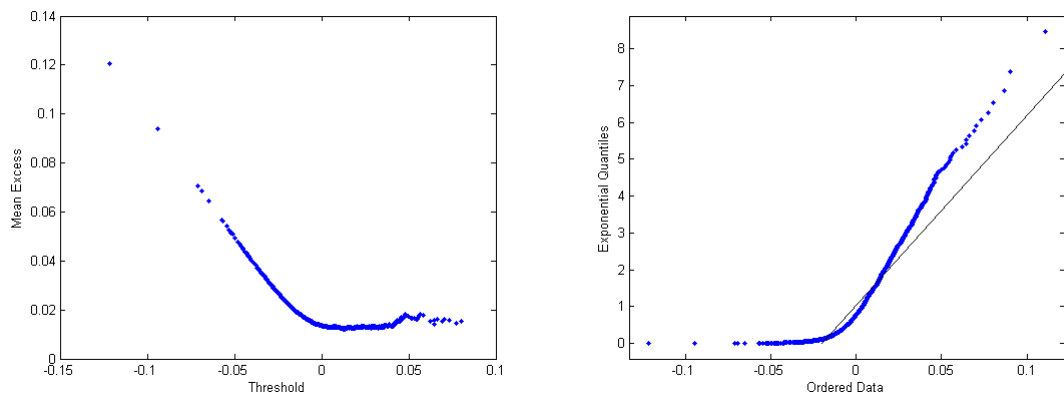


Figure 3.11 : ME (left) and QQ (right) plots of BIST-100 for the left tail, 2004 - 2013.

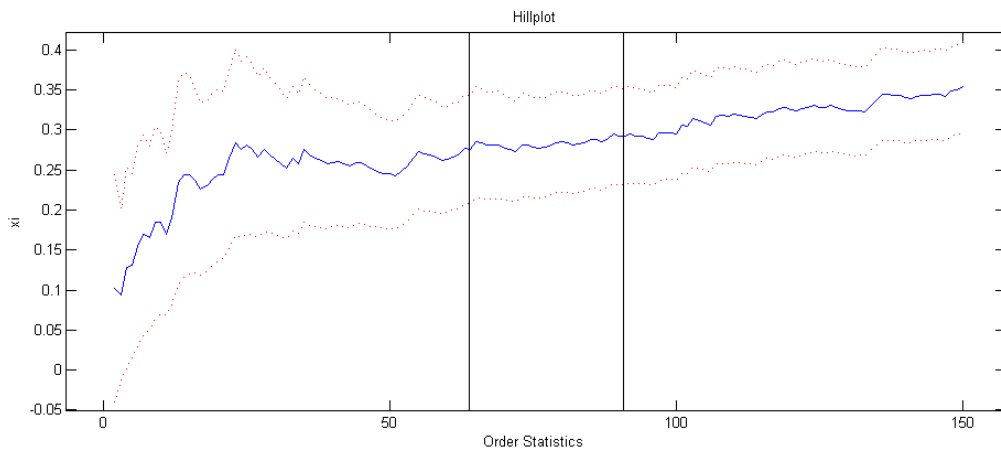


Figure 3.12 : Hill plot of BIST-100 for the left tail, 2004 - 2013.

The important part of the analyzing BIST-100 return distribution with the corresponding right tail is that the graphs which are plotted for the negative returns can be used to explain losses by the means of the extreme value theory. The ME-plots are presented at the left panel of the figure 3.8 and figure 3.11. They have positive

slopes for threshold values greater than approximately 0.05 at the right and left tail regions which indicates fat-tail for the logarithmic BIST-100 returns distributions. Moreover, the QQ-plots are presented in the right panel of the figure 3.8 and figure 3.11. We observe the concave departures from linearity at the tail regions which are also confirmed the fat-tailness of the distributions. On the other hand, the Hill-plots of the data with a 0.95 confidence interval are presented in figure 3.9 and figure 3.12. These graphs exhibit that shape parameters ξ estimate approximately between 0.23 and 0.26, between 0.26 and 0.29 at the relatively stable region enclosed by rectangular, respectively. These values imply power-decaying tail and also fat-tail. The power-decaying tail with an exponent tail index α varies approximately between 3.8 and 4.3, between 3.4 and 3.8 for the right and left tail respectively.

3.3 3D Dynamics of the Average Logarithmic Stock Return, Interest Rate and Speed of Mean Reversion Variables

We analyze the logarithmic stock return behaviors with respect to some of the model parameters especially for various interest rates (r) and speed of mean reversion (κ) when the stock variance (θ) increases or decreases. We perform simulations by using the same brownian motions at each analysis to make a more precise comparison. For example, we make an analysis for the following parameters $r = 2.5\%, 5\%, 10\%, 15\%$, $\kappa = 0.1, 1, 2, 3, 4, 5$ while stock variance changes θ from 0.2 to 0.3, from 0.3 to 0.4 and from 0.4 to 0.5, and vice versa at our analyses.

We obtain 3D graphics of the average logarithmic stock return, interest rate and speed of mean reversion as are in figure 3.13 and figure 3.14. In the both panels of the figure 3.13, the average logarithmic stock return increases as interest rate and speed of mean reversion increase.

Similarly, in figure 3.14, the average logarithmic stock return increases as interest rate increases for all values of κ . On the other hand, the average logarithmic stock return increases as the speed of mean reversion increases for larger values of κ ($\kappa \geq 2$), while it drops for $0.1 \leq \kappa < 2$. The results in figure 3.14 are in the line of the findings in [41] and the all analysis results are almost parallel to the results in Duran and İzgi [31].

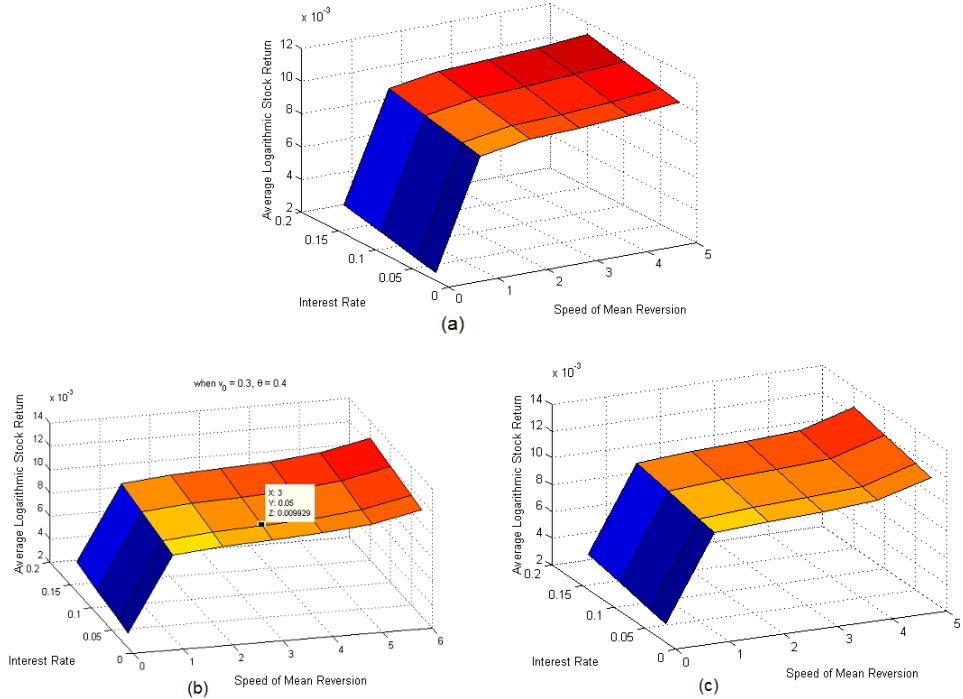


Figure 3.13 : The average logarithmic stock return for $\xi = 0.1$ when the variance of the stock increases: (a) $v_0 = 0.2, \theta = 0.3$, (b) $v_0 = 0.3, \theta = 0.4$, and (c) $v_0 = 0.4, \theta = 0.5$.

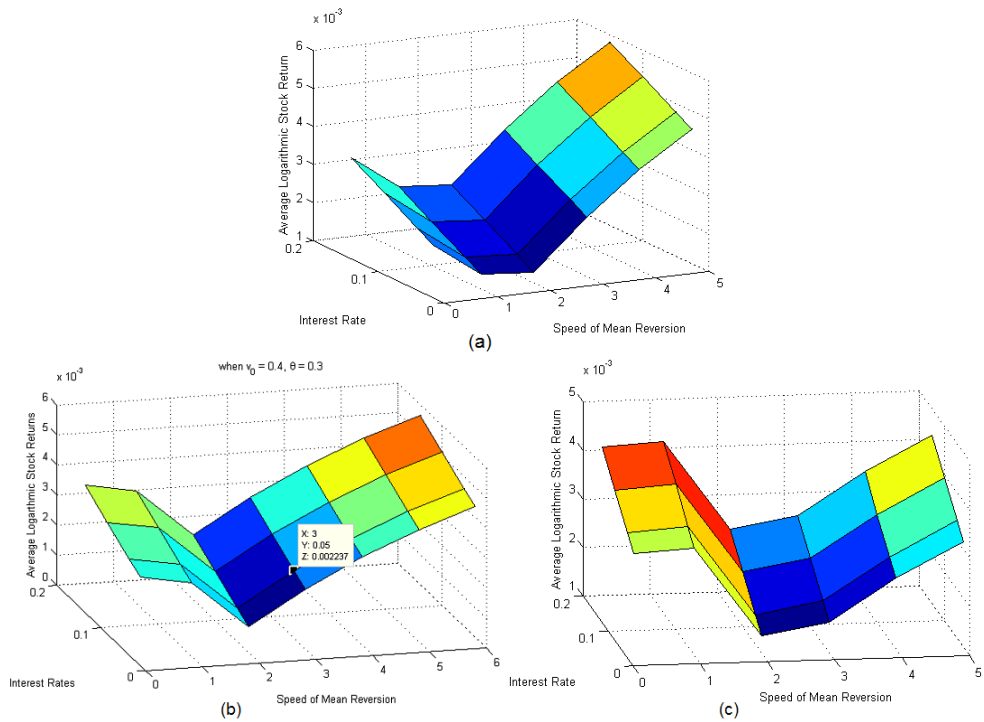


Figure 3.14 : The average logarithmic stock return for $\xi = 0.1$ when the variance of the stock decreases: (a) $v_0 = 0.3, \theta = 0.2$, (b) $v_0 = 0.4, \theta = 0.3$, and (c) $v_0 = 0.5, \theta = 0.4$.

3.4 Comovement and Polarization of Interest Rates and Daily Returns

While daily interest rates in Turkey had large oscillations at high levels between 1996 and 2002, they decreased slowly relatively lower levels with smaller oscillations between 2002 and 2013 according to Central Bank of the Republic of Turkey, as seen in figure 3.15.

By using the methodology having time-dependent return correlation matrices to measure the time dependent polarization [42], we observe that the polarization of BIST-100 and interest rates increases from 2010 to 2011, later it levels off at a relatively high level between 2011 and 2012, and then the polarization decreases slowly in 2013.

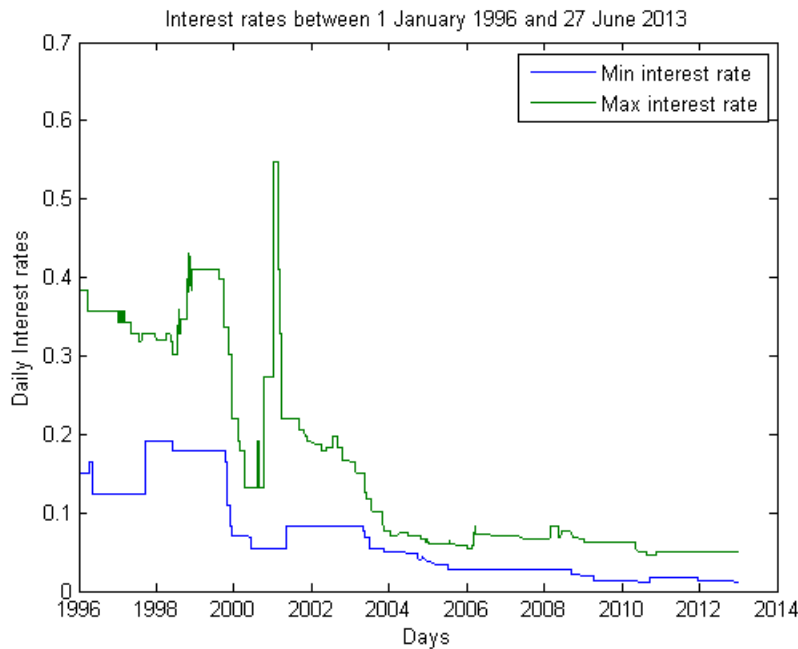


Figure 3.15 : Daily Interest Rates, 1996 - 2013.

Moreover, oscillations of interest rates between 2010 and 2013 are presented in figure 3.16. On the other hand, figure 3.17 shows the comovement and polarization of BIST-100 versus interest rates from May 31, 2010 to June 17, 2013.

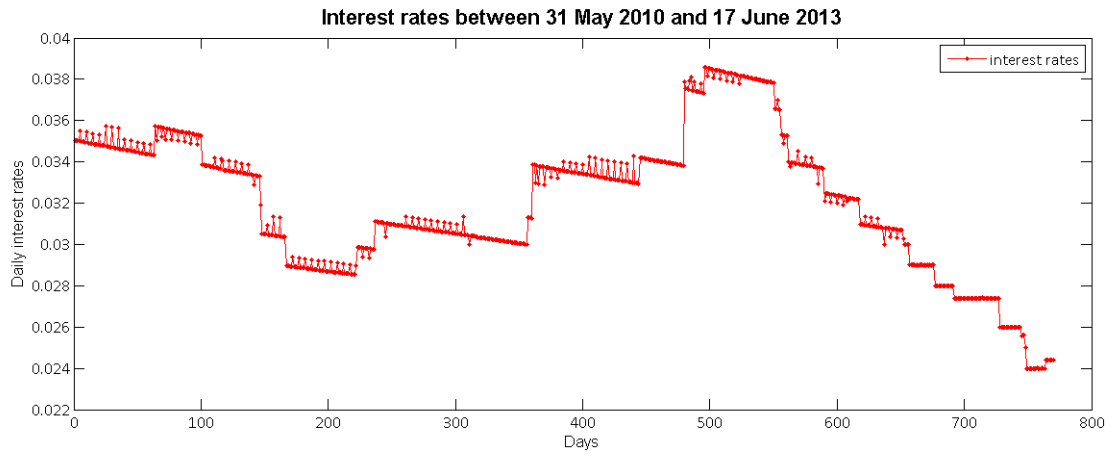


Figure 3.16 : Daily Interest Rates, 2010 - 2013.

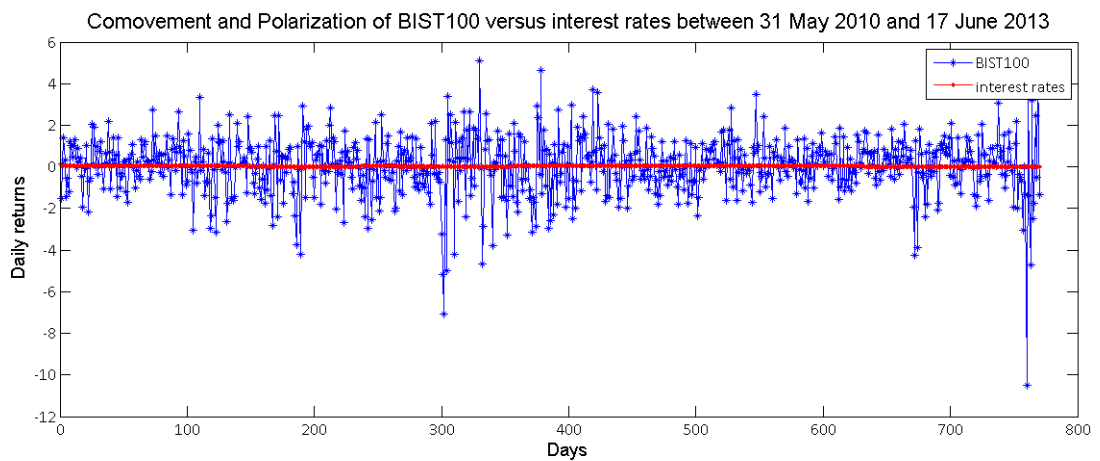


Figure 3.17 : Bist100 vs Interest Rates.

4. JUMP DIFFUSION VS MERTON-BLACK SCHOLES MODELS

Our goal in this chapter is to analyze and compare the behavior of solutions for Merton-Black Scholes and Merton's Jump Diffusion models [4, 5] with respect to the impression matrix norm [6] and extreme value theory [7]. Although there are many studies on MBS and MJD models in the literature, comparisons of their behavior of solutions have not been done by using their extreme values and impression matrix norm together in order to represent jump parameters' effects more easily. Moreover, we occasionally come face with the jump situations at the financial market. It is really hard to estimate and explain abnormal price changes (i.e. jumps, sudden upsurges or other cases, see [43]). For this purpose, we need a useful model which reflects the jumps effect at the security. On the other hand, the underlying stock dynamics are generally described by a stochastic process with a continuous sample path. By their nature, jumps are cutting part of the continuity cases. As a result of the fact that the model generated by a combination of both continuous and jump process is called jump-diffusion process. Therefore, it is challenging to compare the pure diffusion model and jump diffusion model using impression matrix norm (IMN) and extreme value theory (EVT) perspective [8].

4.1 Behavioral Comparisons of Merton Jump Diffusion and Merton-Black Scholes Models

At this section, we discuss advantage and limitations of Merton Black Scholes and Merton's jump diffusion models caused by jump effects. It is noted at Merton's pioneer papers, which has been written about jump diffusion model in 1976 [5], that Merton-Black Scholes model reflects variations of the market situations in a short interval of time as the stock price can only change a small amount. Therefore, it is not able to reflect the fluctuations of the price as it is in the real market. For this purpose, Merton extended the Merton-Black Scholes (MBS) diffusion model to a model that also has a jump component which is called Merton's Jump Diffusion model (MJD) and

allows for a positive probability of a stock price change of extraordinary magnitude in a short or long interval of time [5]. There are different types of the jumps in the literature, for example, Ait-Sahalia and Jacod have extensive work on small and large jumps in their paper [44]. We consider jump situations at our analyses as it is in the real market (i.e. except economic crisis, crashes etc.) when there are only finitely many jumps in each finite time interval in the market. Hanson and Westman has studied parameter estimation problem, which is one of the important part for the jump diffusion applications, for jump-diffusion models at their paper, comprehensively [45]. For this purpose, we focus on mean and variance of the jump and analyze their effects onto behavior of the solutions at the finite time interval via IMN and EVT.

For example, we choose the following model parameters: $t = 0$ (the initial time), $S(0) = 10$ (the initial stock price), $T = 1$ (terminal time), $N = 1000$ (the number of paths), $\mu_S = 0.05$ (expected return rate), $\sigma_S = 0.2$ (volatility parameter of stock process), $\lambda = 25$ (jump intensity), while we perform simulations for extensive analyses. We conduct simulations on the same paths to compare MBS and MJD models more precisely and present effects of the jumps, which are lognormally distributed random variables with mean $\mu_X = 0$ and variance $\sigma_X^2 = 1$, by using the jump-adapted approximation method [12, 23].

Since it is hard to see their parallel behavior until the first jump occurs, we choose jump intensity $\lambda = 2$ to present variations at the model caused by the jump more explicitly (see figure 4.1). Moreover, we present logarithmic stock price graphics and their histograms with the best fitted normal distribution for each model that obtained from one thousand simulations according to the above parameters in figure 4.2 and figure 4.3, respectively.

Generally the changes in stock prices from MBS model are smaller than those of MJD model, in the same finite time interval. Figure 4.2 displays that the logarithmic stock prices coming from MBS model vary between 1.6 and 3 while those of MJD fluctuate extraordinary magnitude between -15 to 25 in the same time interval (i.e. between 0 to 1), due to jump effects. This situation is also supported by their distributions in figure 4.3. We will investigate the jump effects using various parameters more quantitatively in the following sections.

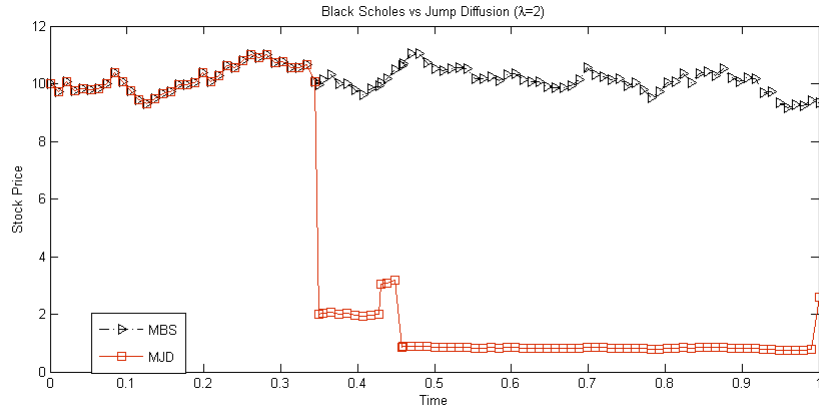


Figure 4.1 : One path of MBS and MJD while $\lambda = 2$.

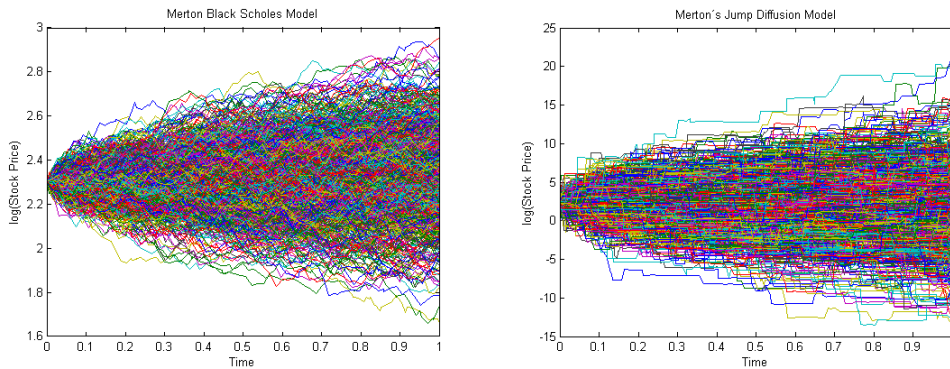


Figure 4.2 : One thousand simulation paths of MBS (left) and MJD (right) while $\mu_X = 0$ and $\sigma_X = 1$ for MJD.

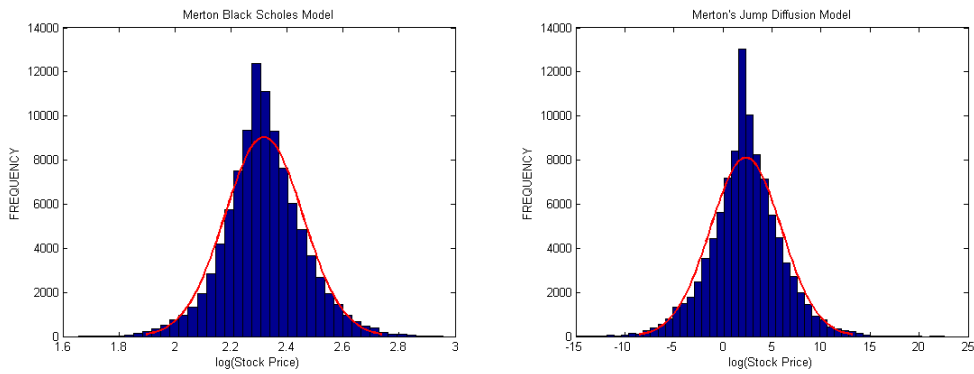


Figure 4.3 : Histograms of MBS (left) and MJD (right) with the best fitted normal distribution while $\mu_X = 0$ and $\sigma_X = 1$ for MJD.

4.1.1 Extensive behavioral analysis of the jump

We choose jump terms from log-normal distribution as it is considered by Merton (X_i 's are from $\mathbb{LN}(\mu, \sigma^2)$, see [5]) so that stock price has log-normal distribution, as well. Moreover, we focus on analysis of their behavioral effects at the solutions (such as logarithmic stock price) especially for different jumps' mean and variance values. We

also present extreme value analysis (i.e. skewness, fat-tailness) based on extreme value theory. Here some of the graphics are presented which obtained from simulations for MJD model for different μ_X and σ_X by using the given parameters at the previous section. We note that the mean and variance values are just chosen as an example for the different four scenarios at this application, and it can be done for different values for each scenario, as well.

- For the negative mean value of the jump parameter : ME-plot, QQ-plot and Hill plot are presented for the left tail (prices multiplied by -1) of the distribution.

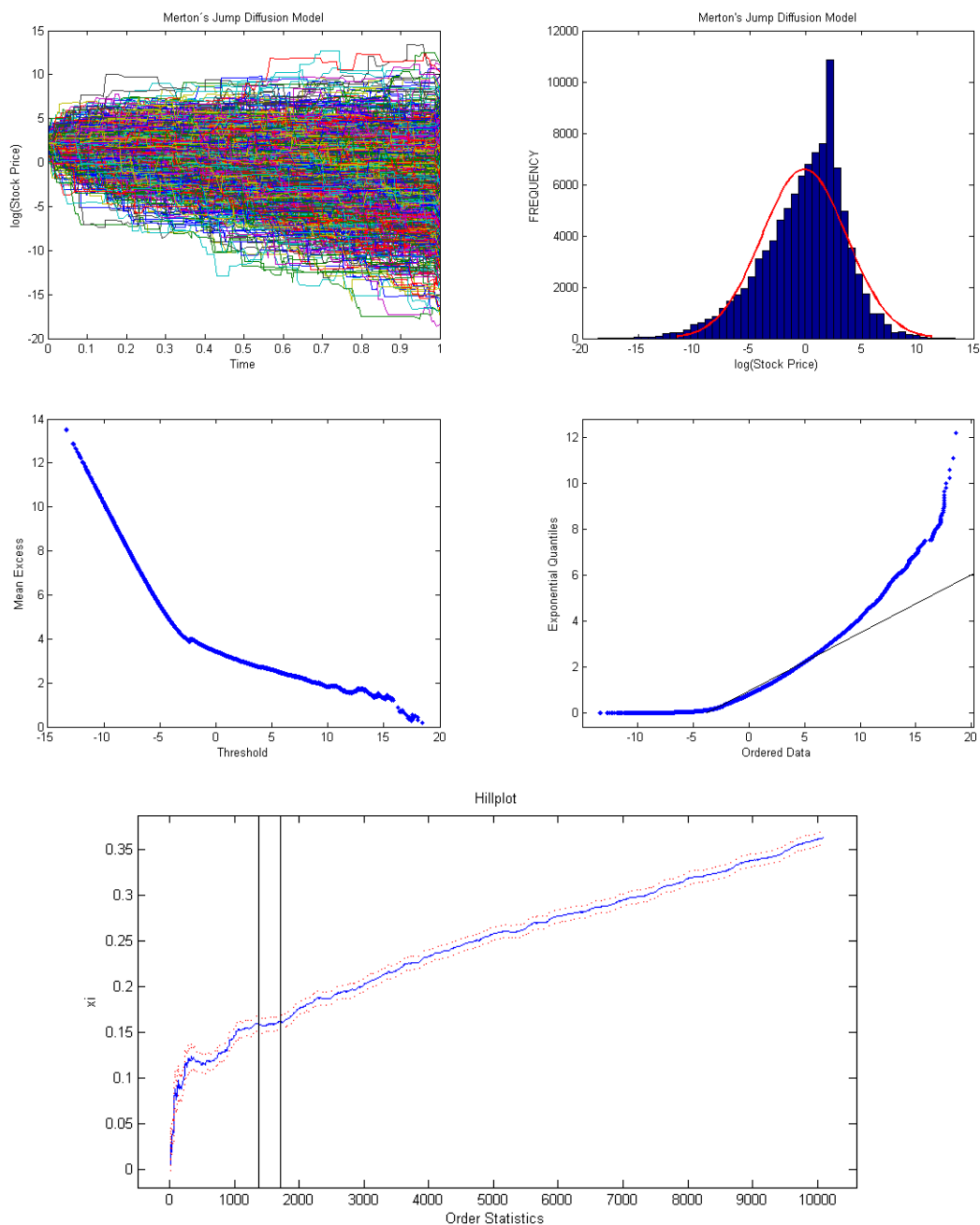


Figure 4.4 : Solutions behavior of MJD while $\mu_X = -0.2$ and $\sigma_X = 1$.

- For the positive mean value of the jump parameter :

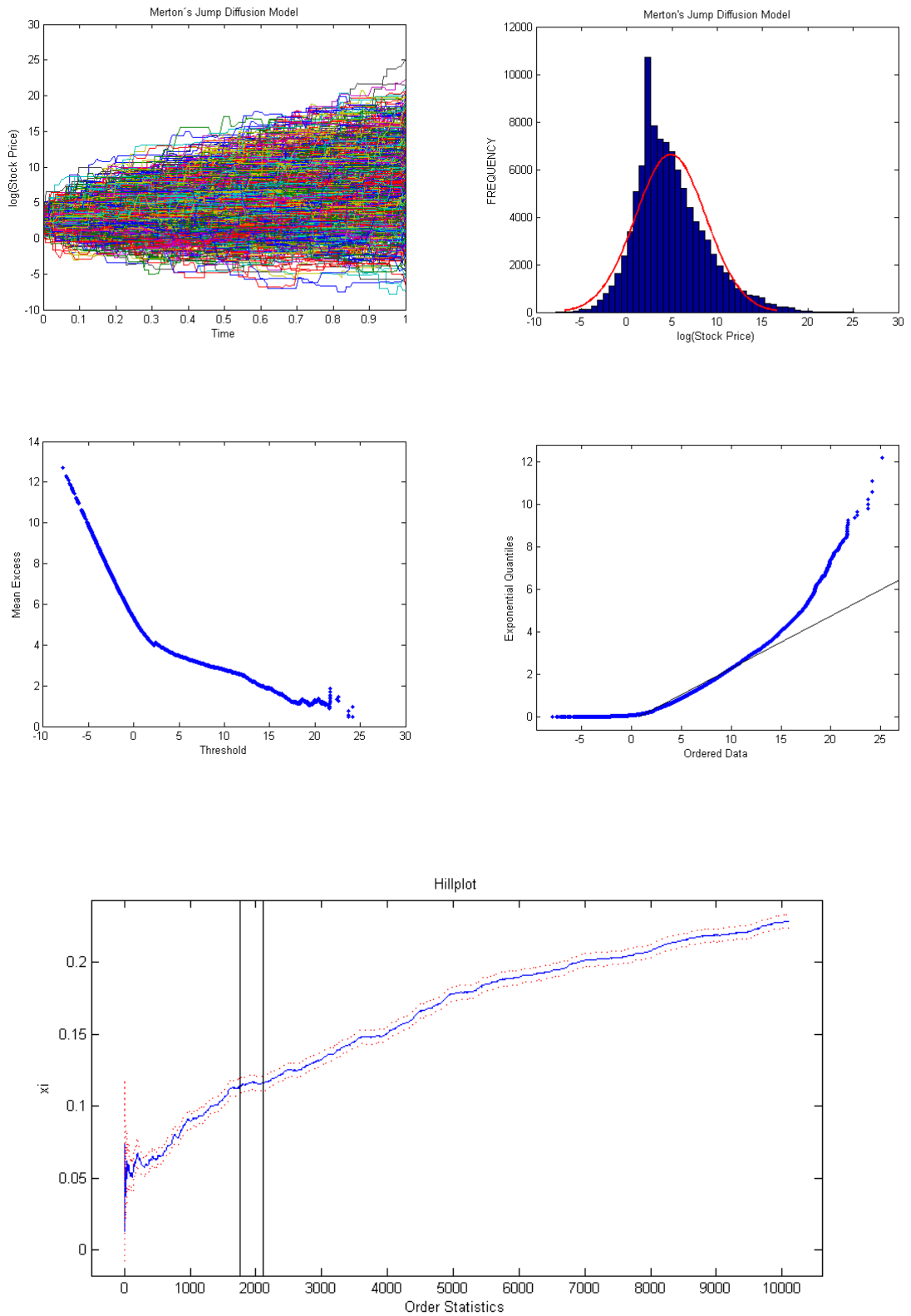


Figure 4.5 : Solutions behavior of MJD while $\mu_X = 0.2$ and $\sigma_X = 1$.

- Extensive analyses for the incremental variance values of the jump parameter :

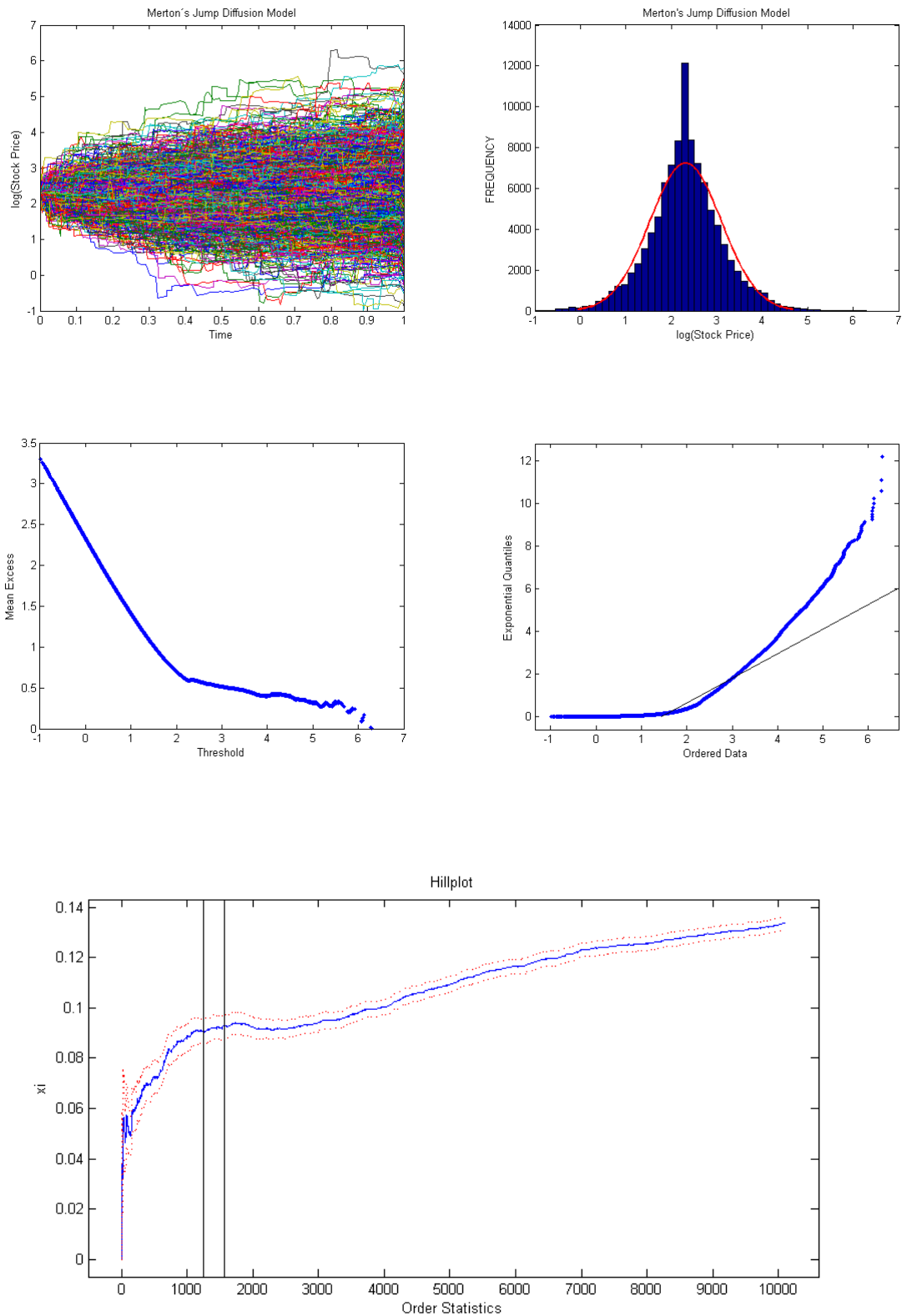


Figure 4.6 : Solutions behavior of MJD while $\sigma_X = 0.22$ and $\mu_X = 0$.

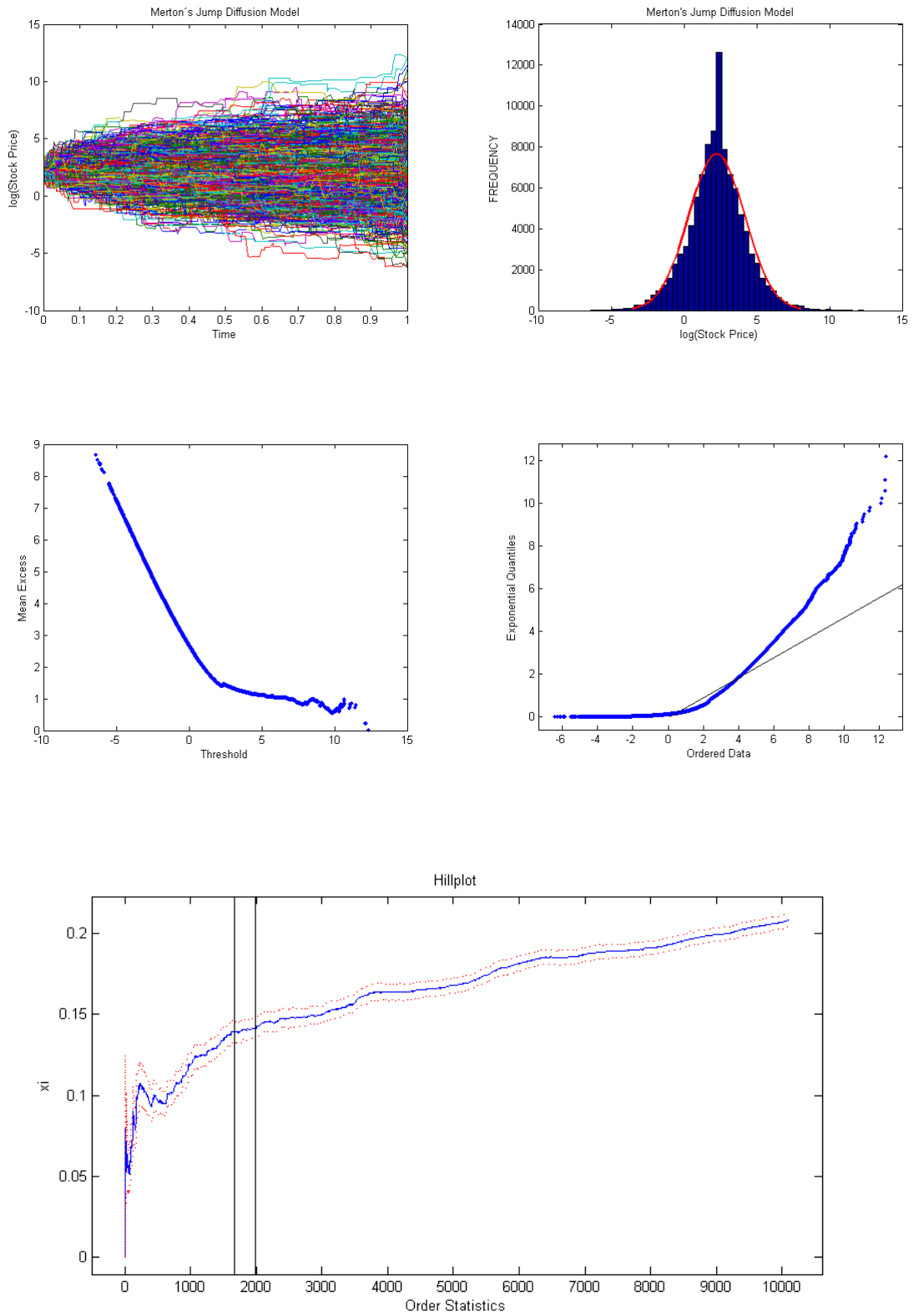


Figure 4.7 : Solutions behavior of MJD while $\sigma_X = 0.55$ and $\mu_X = 0$.

4.2 Summary of the Extensive Behavioral Analyses

After the all simulation results, we are at the position to interpret behavior of the logarithmic stock price more easily under the consideration of the histograms, Mean Excess plots (ME-plots), Quantile-Quantile plots (QQ-plots) and Hill-plots of the logarithmic stock price distributions. We present approximate statistical values of the logarithmic stock price distribution in table 4.1 which obtained from simulations for MBS model using the related parameters. Moreover, we obtain table 4.2 and table 4.3 for the quantitative information for MJD model to present effects of the jumps more explicitly when we compare them with the MBS model's statistical values.

Table 4.1 : MBS: Statistics for the distribution of logarithmic stock price.

Merton Black Scholes Model					
Min	Mean	Max	Standard deviation	Skewness	Kurtosis
1.674	2.307	2.94	0.3795	0.0891	3.9930

First of all, we see the effects of the jumps from standardized moments values when we compare table 4.1 with table 4.2 and table 4.3, clearly. Such that, the minimum, mean and maximum values of the logarithmic stock price distributions have sensitivity with jump. We observe that they present parallel behavior with respect to the incremental jump's mean for the constant variance value of the jump (see table 4.2).

On the other hand, we present that the minimum values of the distributions represent inverse relation as jump's variance values increase for the constant mean of the jump. Moreover, the maximum values behave almost parallel with their behavior (see table 4.3). Although the logarithm stock price distribution for the MBS model has relatively low standard deviation level, it also has relatively high standard deviation levels for the different mean and variance values of the jump at the MJD model (see table 4.2 and table 4.3).

The other most important observation is that the distribution has negative skewness for the negative mean of the jump while it has positive skewness for the positive mean of it (see figure 4.4 and figure 4.5). This is consistent with the literature results for the MJD model [43, 46], and its skewness is $\frac{\lambda\mu_X(\mu_X^2+3\sigma_X^2)}{(\sigma_S^2+\lambda(\sigma_X^2+\mu_X^2))^{\frac{3}{2}}\sqrt{t}}$ which can be obtained for MJD model. Here σ_S^2 and σ_X^2 are variances of the stock price and jump respectively while μ_X is the mean parameter of the jump.

Table 4.2 : MJD: Statistics for the distributions of logarithmic stock price for μ_X while $\sigma_X = 1$.

μ_X	Min	Mean	Max	Standard deviation	Skewness	Kurtosis
-0.2	-18.26	-2.603	13.06	9.318	-0.6641	3.8121
0	-14.47	3.847	22.17	10.9	0.0604	4.4027
0.2	-7.534	8.62	24.77	9.612	0.7539	3.8631

Table 4.3 : MJD: Statistics for the distributions of logarithmic stock price for σ_X while $\mu_X = 0$.

σ_X^2	Min	Mean	Max	Standard deviation	Skewness	Kurtosis
0.05	-0.9109	2.658	6.227	2.123	0.0494	4.0928
0.3	-6.235	2.966	12.17	5.474	0.0111	3.9811
1	-15.83	2.492	20.81	10.9	0.1355	4.3855

When we compare the kurtosis values of the MBS model and MJD model, we see that they have relatively high kurtosis values. Therefore, it may be interpreted as they have high peaks. Although the kurtosis value is generally necessary sign, when it is greater than 3, for the fat-tailness of the related distributions, it is not sufficient condition to decide about fat-tailness of the distribution just by using this magnitude [7, 33, 40]. For this purpose, we use extreme value theory tools such that ME-plot, QQ-plot and Hill-plot while we analyze fat-tailness for the distribution of the logarithm stock price. The extreme value analyses results of the MJD model for the different jump parameters are already displayed in figures 4.4-4.7. Here in figure 4.8, we present graphics for the MBS model obtained from extreme value analysis.

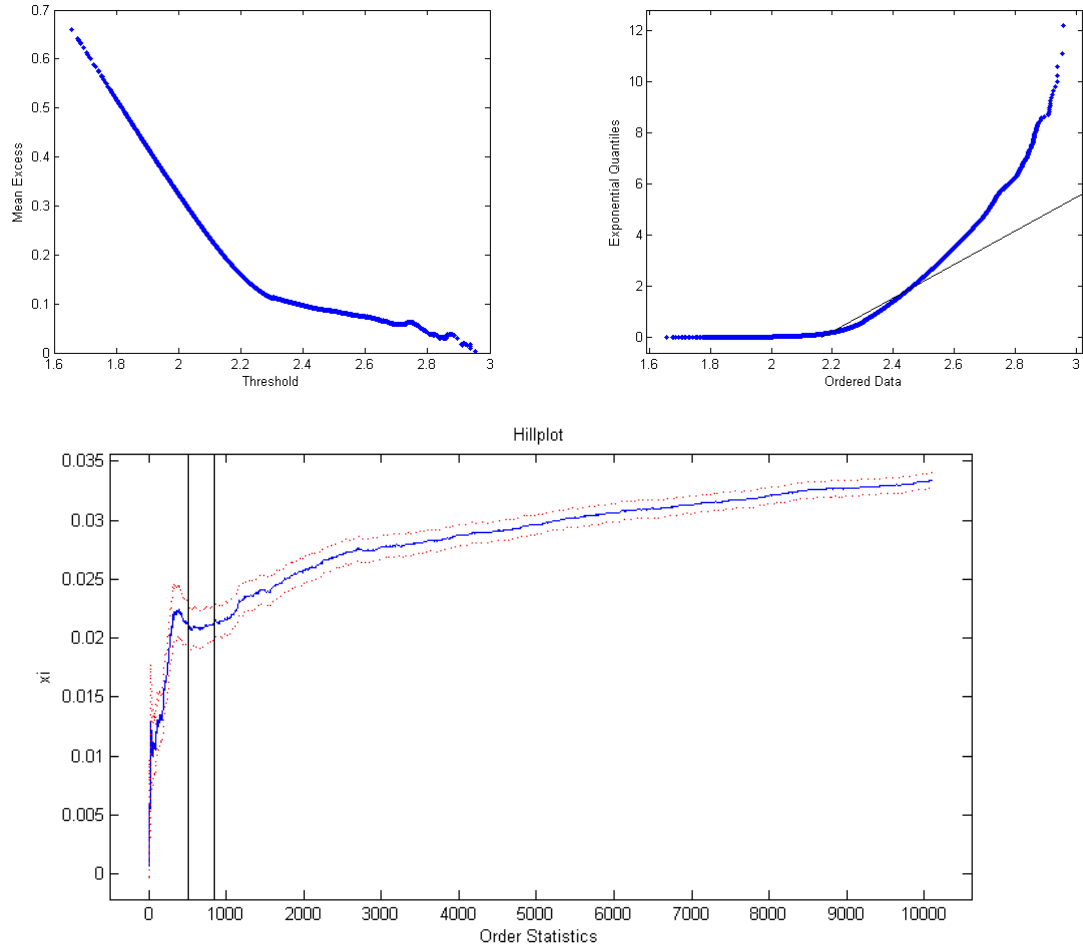


Figure 4.8 : Extreme value analysis of the MBS model: ME-plot (top-left), QQ-plot (top-right) and Hill-plot (bottom).

ME-plot for the left tail analysis (prices multiplied by -1) in figure 4.4 and the all other ME-plots for the MBS and MJD models have positive slope at the tail regions which indicate a heavy right tails (it indicates a heavy left-tail for the negative mean value of the jump parameter, see figure 4.4) for the logarithmic stock price distributions. Moreover, the QQ-plots against the exponential distribution, where the sufficiently large concave departure from linearity is presented at the right tail region (at the "left tail region" for the negative mean value of the jump parameter analysis), support evidences of fat-tailness of the underlying distributions. In addition, we observed from the all analysis results that the shape parameters ξ are all positive ($\xi > 0$) at the relatively stable regions, which are indicated with the rectangular, in the Hill-plots obtained for the logarithmic stock price distributions with a 0.95 confidence interval. These results imply that a power-decaying tail and also heavy tail [7, 33, 40].

4.3 Application of Impression Matrix Norm for Jump Process

Interpretation of the dynamic large data sets is important in financial market in order to make exact and correct investment decision quickly. Financial instruments' prices are generally depend on lots of variables at the same time. Controlling of them is the one of the hardest situations when determining the investment strategy.

We consider a 2-dimensional matrix having time and different scenario dimensions where matrix entries are market prices. As an application of 2-dimensional norms we use moving matrix which we define in the chapter 2. Also, we use impression matrix norm (IMN) as a norm of the moving matrix with respect to time. IMN is generated by evaluating the norm of the matrix at each related time sub-interval [6, 27]. We represent usefulness of the IMN for the 3-D matrix in the chapter 2, comprehensively (see also [6, 27]). Here, we use IMN for 2-D matrix which gives us a good picture of all the 2-D matrix data, and reflects model properties to understand and interpret 2-D matrix more easily.

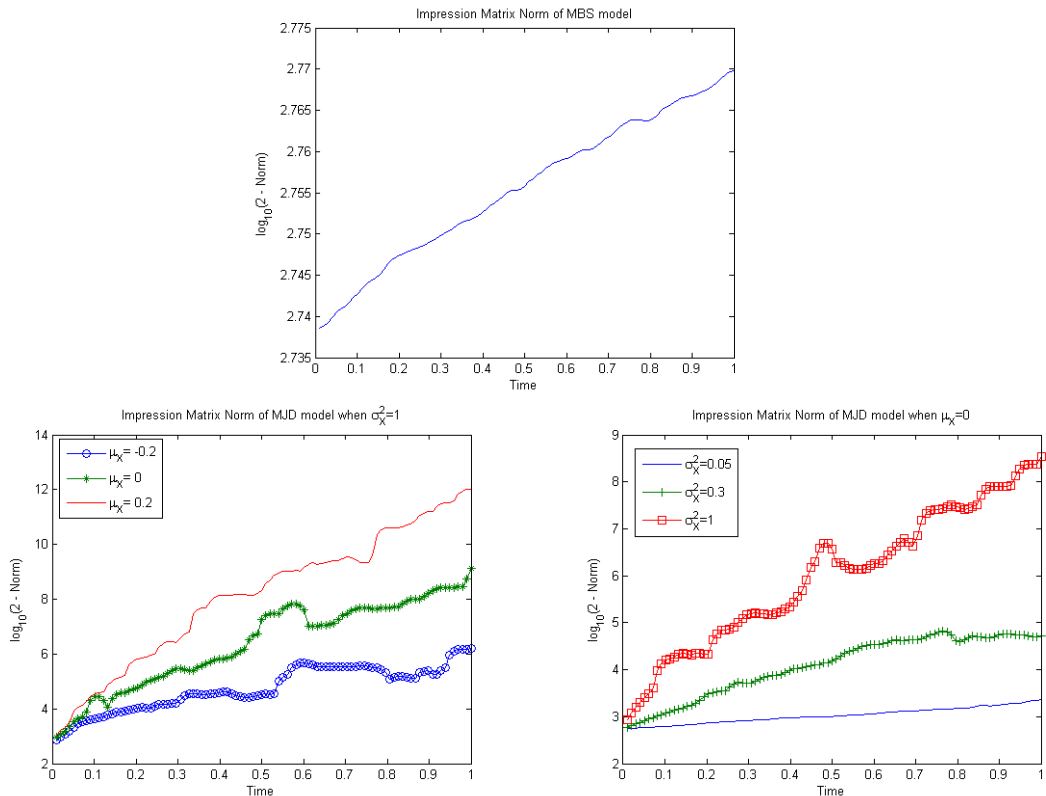


Figure 4.9 : Impression Matrix Norms of the MBS model (top) and MJD for different means (bottom-left) and variances (bottom-right) of the jump.

After we perform simulations for a given parameters in section 4.1, we obtain 2-dimensional expectation matrix M ($M \in \mathbb{C}^{100 \times 1000}$). Now, for instance, let us select the length of time sub-interval as 0.01 year (i.e. approximately 2.53 trading days) and the number of time sub-interval as 3. After that, we use impression matrix norm in the 2-norm for M to analyze and quantify price impression approximately and obtain the graphs in figure 4.9.

These graphs reflect almost the expected behaviors comes from the naturality of the models especially for the Merton's jump diffusion model. Moreover, IMN presents relationship between effect of the mean (and variance) of the jump parameters and price fluctuations, explicitly. Furthermore, we show that prices have almost parallel behavior with jump's variance and mean magnitudes using impression matrix norm in the bottom panel of the figure 4.9.

5. CONCLUSIONS AND RECOMMENDATIONS

We find that defining 3-dimensional matrix norms, summarizing large financial data set and quantifying market impression with respect to several variables together are useful. We obtain a proxy for time evolution of market impression value, and perform simulations for various model parameters. We see that using the volatility in terms of extreme values makes it easy to evaluate volatilities when we perform simulations with the large real data set. According to the simulation results, Heston stochastic volatility model can not promise much things at the long time interval since the initial information lose their effect by the time.

It is challenging to compare the advantages and limitations of the higher order SDE-solvers. We present that there is inverse relationship between speed of convergence of the methods and impression matrix norm (IMN) values while using the annual volatilities having extreme values as in the line of literature. When we examine the numerical methods using IMN in terms of their trade-offs, although SRK takes more time, it worths to prefer SRK to Euler-Maruyama method and Milstein method just because that SRK's lower cumulative error is important for our financial applications.

We obtained from the results in table 2.6 that it does not matter which method is used for the applications having such relatively low volatility cases with respect to the robustness. On the other hand, we suggest Euler Maruyama method because of its lowest cost for daily volatility usage or market situations at such low volatility levels.

Moreover, we obtained valuable results for the solution behaviors of the Heston stochastic volatility model from the various model parameter analyses. We present relationships between speed of the mean reversions and the extreme values of the logarithmic stock returns obtained from Heston stochastic volatility model for the positive and negative correlation coefficients. We show that the logarithmic stock return distributions not only for Heston model but also for BIST - 100 index have fat-tails and high-peaks by using the extreme value theory. Consequently, we obtained

for some of the model parameters that Heston model reflects high-peaks and fat-tails for the logarithmic stock returns distribution with various behaviors.

In addition, Heston stochastic volatility model may capture comovement of stock price return and interest rates. We observe that the average logarithmic stock return rises gradually as interest rate and speed of mean reversion increase, while stability of stock market decreases, according to the Heston model. Actually, interest rates were decreased around 2008 and stock prices increased gradually in US stock markets, unlike the Heston model suggests. Borsa Istanbul experienced similar situations between 2002 and 2013, and this is a kind of polarization of stock price return and interest rates for some sufficiently large time intervals. Krugman, 2008 nobel laureate in economics, appreciates lower interest rates in order to encourage investments (see Krugman [47]). The polarization may be explained by Krugman's this argument.

Furthermore, the Heston model predicts that the average logarithmic stock return increases as interest rate goes up for all values of κ , when the stability of stock market gets better. On the other hand, the average logarithmic stock return increases as the speed of mean reversion increases for larger values of κ , while it drops for $0.1 \leq \kappa < 2$ and this is consistent with the arguments of Avellaneda and Jee [41].

It is valuable to prefer a more realistic model which capture all parameters' effect in a short or long time interval. We believe that MJD model may reflect much more variety of market situations with suitable jump parameters based on our quantitative analysis using extreme value tools such that QQ-plot, ME-plot and Hill plot. We illustrate some model parameters effects at the logarithmic stock price distributions for the Merton-Black Scholes and Merton's Jump Diffusion models. Moreover, we success to show fat-tailness and high peak of the distributions, which may happen in the real stock market, obtained by the simulations using extreme value theory and standardized moments values. In particular, the relationship between the jump parameters (mean and variance of the jump parameter) and the logarithmic stock price distribution are presented by means of the fat-tailness and high peak sense. These extreme situations may not materialize at the Merton-Black Scholes model as much as the Merton's jump diffusion model (see figure 4.2) in a same time interval. Because extreme situations are generally rare events, one may consider MBS model, at first glance. However, the lose or gain amount is considerable during the extreme events. We suggest traders using

MJD model in order to catch and control the extreme behavior of the price fluctuations, so that they can avoid to generate potential arbitrage cases at their investment for the others by this distinguished property of the MJD model.

Finally, we show that applications of the impression matrix norm for the Merton's jump diffusion and Merton-Black Scholes models are also useful as it is shown at the real data applications for Heston model. IMN can be alternative tool to examine the presence of the jump at the empirical or real data applications. One of our contribution is that IMN can be used for the real stock market especially at the estimation for the price behavior in the incomplete markets which reflect jumps or any other anomalies that are caused by jumps. The relationship between incomplete market and jumps is also consistent in the line of the findings in Ait-Sahalia and Jacod [44]. For this purpose, we suggest the practitioners using MJD model, while they are modeling any security, since theoretical and numerical results show that MBS model can not reflect most abnormal situations at the market as much as MJD model. Therefore, the market players may mislead by using MBS model instead of MJD model. Moreover, even there is sudden upsurges in prices, applications of the IMN for the jump diffusion model can make feasible to control lots of variable together. This is one of the important parts of the investment strategies.

REFERENCES

- [1] **Duran, A. and Caginalp, G.** (2007). Overreaction Diamonds: Precursors and Aftershocks for Significant Price Changes, *Quantitative Finance*, 7(3), 321–342.
- [2] **Duran, A.** (2011). Stability Analysis of Asset Flow Differential Equations, *Applied Mathematics Letters*, 24(4), 471–477.
- [3] **Heston, S.** (1993). A Closed-Form Solution for Options with Stochastic Volatility with Applications to Bond and Currency Options, *Review of Financial Studies*, 6(2), 327–343.
- [4] **Black, F. and Scholes, M.** (1973). The Pricing of Options and Corporate Liabilities, *Journal of Political Economy*, 81, 637–654.
- [5] **Merton, R.** (1976). Option Pricing When Underlying Stock Returns are Discontinuous, *J. Financial Economics*, 3, 125–144.
- [6] **Duran, A. and İzgi, B.** (2015). Application of the Heston Stochastic Volatility Model for Borsa Istanbul Using Impression Matrix Norm, *Journal of Computational and Applied Mathematics*, 281, 126–134.
- [7] **İzgi, B. and Duran, A.** (submitted, 2015). 3D Extreme Value Analysis for Stock Return, Interest Rate and Speed of Mean Reversion.
- [8] **İzgi, B. and Duran, A.** (submitted, 2015). Behavioral Comparisons of Merton’s Jump Diffusion and Merton-Black Scholes Models Using Extreme Value Theory and Impression Matrix Norm.
- [9] **Karatzas, I. and Shreve, S.E.** (1991). *Brownian Motion and Stochastic Calculus*, Springer, second edition.
- [10] **Mao, X.** (2007). *Stochastic Differential Equations and Applications*, Woodhead Publishing, second edition.
- [11] **Cvitanic, J. and Zapatero, F.** (2004). *Introduction to the Economics and Mathematics of Financial Markets*, MIT press.
- [12] **Glasserman, P.** (2004). *Monte Carlo Methods in Financial Engineering*, Springer, New York.
- [13] **Cox, J.C., Ingersoll, J.E. and Ross, S.A.** (1985). A Theory of the Term Structure of Interest Rates, *Econometrica*, 53, 385–407.
- [14] **Feller, W.** (1951). Two Singular Diffusion Problems, *Annals of Mathematics*, 54, 173–182.

- [15] **Maruyama, G.** (1955). Continuous Markov Processes and Stochastic Equations, *Rend. Circ. Mat. Palermo*, 4, 48–90.
- [16] **Milstein, G.** (1974). Approximate Integration of Stochastic Differential Equations, *Theor. Prob. Appl.*, 19, 557–562.
- [17] **Burrage, K. and Burrage, P.** (1996). High Strong Order Explicit Runge-Kutta Methods for Stochastic Ordinary Differential Equations, *Appl. Numer. Math.*, 22, 81–101.
- [18] **Burrage, K., Burrage, P. and Mitsui, T.** (2000). Numerical Solutions of Stochastic Differential Equations-Implementation and Stability Issues, *Journal of Computational and Applied Mathematics*, 125, 171–182.
- [19] **Kloeden, P., Platen, E. and Schurz, H.** (2003). *Numerical Solution of SDE Through Computer Experiments*, Springer, Berlin.
- [20] **Rossler, A.** (2010). Runge Kutta Methods for the Strong Approximation of Solutions of Stochastic Differential Equations, *SIAM Journal on Numerical Analysis*, 48, 922–952.
- [21] **Shreve, S.E.** (2004). *Stochastic Calculus for Finance II: Continuous-Time Models*, Springer.
- [22] **Hanson, F.B.** (2007). *Applied Stochastic Processes and Control for Jump-Diffusions: Modeling, Analysis and Computation*, SIAM.
- [23] **Platen, E. and Liberati, N.B.** (2010). *Numerical Solutions of Stochastic Differential Equations with Jumps in Finance*, Springer, Berlin.
- [24] **Trefethen, L.N. and Bau III, D.** (1997). *Numerical Linear Algebra*, SIAM.
- [25] **Royden, H.** (1988). *Real Analysis*, Macmillan, third edition.
- [26] **Duran, A. and Bommarito, M.** (2011). A Profitable Trading and Risk Management Strategy Despite Transaction Cost, *Quantitative Finance*, 11, 829–848.
- [27] **Duran, A. and İzgi, B.** (2014). *Solution Behavior of Heston Model Using Impression Matrix Norm*, volume 87, Springer Proc. in Mathematics & Statistics, Springer Switzerland, doi 10.1007/978-3-319-06923-4-20, 215-221.
- [28] **Parkinson, M.** (1980). The Extreme Value Method for Estimating the Variance of the Rate of Return, *The Journal of Business*, 53, 61–65.
- [29] **Duran, A.** (2009). Sensitivity Analysis of Asset Flow Differential Equations and Volatility Comparison of Two Related Variables, *Numer. Func. Anal. and Opt.*, 30, 82–97.
- [30] **Bodie, Z., Kane, A. and Marcus, A.** (2005). *Investments*, Irwin McGraw-Hill, Boston, MA, sixth edition.

- [31] **Duran, A. and İzgi, B.** (2014). Comovement and Polarization of Interest Rate and Stock Market in Turkey, *Proceedings of Borsa Istanbul Finance and Economics Conference*, ISBN: 978-605-5076-04-7, 130–141.
- [32] **Bommarito, M. and Duran, A.** (2010). Spectral Analysis of Time-Dependent Market-Adjusted Return Correlation Matrix, Available at SSRN: <http://dx.doi.org/10.2139/ssrn.1672897>.
- [33] **Embrechts, P., Kluppelberg, C. and Mikosch, T.** (1997). *Modelling Extremal Events for Insurance and Finance*, Springer-Verlag, Berlin.
- [34] **Reiss, R. and Thomas, M.** (1997). *Statistical Analysis of Extreme Values*, Birkhauser, Basel.
- [35] **Beirlant, J., Teugels, J. and Vynckier, P.** (2004). *Statistics of Extremes: Theory and Applications*, John Willey and Sons.
- [36] **Huisman, R., Koedijk, K., Kool, C. and Palm, F.** (2001). Tail Index Estimates in Small Samples, *Journal of Business and Economic Statistics*, 19, 208–216.
- [37] **Mcneil, A.** (1997). Estimating the Tails of Loss Severity Distributions Using Extreme Value Theory, *ASTIN Bulletin*, 27, 117–137.
- [38] **Gencay, R., Selçuk, F. and Ulugülyağcı, A.** (2003). High Volatility, Thick Tails and Extreme Value Theory in Value-at-Risk Estimation, *Journal of Insurance: Mathematics and Economics*, 33, 337–356.
- [39] **Hill, B.** (1975). A Simple General Approach to Inference About the Tail of a Distribution, *The Annals of Statistics*, 3, 1163–1174.
- [40] **Gencay, R., Selçuk, F. and Ulugülyağcı, A.** (2001). EVIM: A Software Package for Extreme Value Analysis in Matlab, *Studies in Nonlinear Dynamics and Econometrics*, 5, 213–239.
- [41] **Avellaneda, M. and Jee, J.** (2010). Statistical Arbitrage in the U.S. Equities Market, *Quantitative Finance*, 10, 761–782.
- [42] **Duran, A.**, (2013). Over-correlated Markets and Consecutive Overreactions, Book of Abstracts, Borsa Istanbul Finance and Economics Conference, p. 25.
- [43] **Ramezani, C.A. and Zeng, Y.** (1998). Maximum Likelihood Estimation of Asymmetric Jump-Diffusion Processes: Application to Security Prices, Available at SSRN 606361.
- [44] **Ait-Sahalia, Y. and Jacod, J.** (2012). Analyzing the Spectrum of Asset Returns: Jump and Volatility Components in High Frequency Data, *Journal of Economic Literature*, 50(4), 1007–1050.
- [45] **Hanson, F.B. and Westman, J.** (2002). Jump-Diffusion Stock Return Models in Finance: Stochastic Process Density with Uniform-Jump Amplitude, *Proc. 15th International Symposium on Mathematical Theory of Networks and Systems*, 7, 1–7.

- [46] **Matsuda, K.** (2004). Introduction to Option Pricing with Fourier Transform: Option Pricing with Exponential Levy Models, *Ph.D. thesis*, Graduate School and University Center of the City University.
- [47] **Krugman, P.** (2001). Fuzzy Math Returns, *The New York Times*.

CURRICULUM VITAE

Name Surname: Burhaneddin İZGİ

Place and Date of Birth: Diyarbakır, 29.03.1986

Address: ITU, Ayazağa Campus, Faculty of Science and Letters

E-Mail: bizgi@itu.edu.tr, burhan86@gmail.com

B.Sc.: Mimar Sinan University, 2004 - 2008

M.Sc.: Mimar Sinan University, 2008 - 2010

PROFESSIONAL EXPERIENCE AND REWARDS :

- Visiting Researcher, June 2014 - December 2014, Mathematics and Statistics Department, California State University (Sacramento), USA.
- Fellowship from The Scientific and Technological Research Council of Turkey TUBITAK, 2010 - 2015.

PUBLICATIONS ON THE THESIS

- Duran A. and **İzgi B.**, 2015: Application of the Heston Stochastic Volatility Model for Borsa Istanbul Using Impression Matrix Norm, *Journal of Computational and Applied Mathematics*, 281, pp. 126 - 134.
- **İzgi B.** and Duran A., submitted 2015: 3D Extreme Value Analysis for Stock Return, Interest Rate and Speed of Mean Reversion.
- **İzgi B.** and Duran A., submitted 2015: Behavioral Comparisons of Merton's Jump Diffusion and Merton-Black Scholes Models Using Extreme Value Theory and Impression Matrix Norm.
- Duran A. and **İzgi B.**, 2014: Solution Behavior of Heston Model Using Impression Matrix Norm, *Advances in Applied Mathematics, Springer Proc. in Mathematics & Statistics*, DOI 10.1007/978-3-319-06923-4-20, 87, 215-221, Springer Switzerland.
- Duran A. and **İzgi B.**, 2014: Comovement and Polarization of Interest Rate and Stock Market in Turkey, *Borsa Istanbul Finance and Economics Conference (BIFEC), Book of Abstract and Proceedings*, ISBN: 978-605-5076-04-7, pp.130-141, Istanbul, Turkey.

PRESENTATIONS ON THE THESIS

- Duran A. and **İzgi B.**, 2013: Solution Behavior of Stochastic Differential Equations and Impression Matrix Norm, *Joint SIAM and Gulf International Conference on Applied Mathematics*, November 19-21, 2013, Kuwait.

- Duran A. and **İzgi B.**, 2013: Comovement and Polarization of Interest Rate and Stock Market in Turkey, *BIFEC - Borsa Istanbul Finance and Economics Conference*, September 30 - October 1, 2013, Istanbul, Turkey
- **İzgi B.** and Duran A., 2013: Overreaction of Young Investors, *Model Economic Forum*, March 1-3, 2013, Istanbul, Turkey.